

6342

DOC. NO.
NARF-62-14T
FZK-9-179

1

**FIRST OPERATIONAL YEAR
OF THE RTA**

seal

AD No. ~~409~~ 860

DDC FILE COPY

409 860

JUL 1962
RECEIVED
TISIA A

NUCLEAR AEROSPACE RESEARCH FACILITY

operated by

GENERAL DYNAMICS | FORT WORTH

\$ 9.10

DOC. NO.
NARF-62-14T
FZK-9-179

(4) 9.10
(5) 351860

(14) Document
DOC. NO.
NARF 62-14T
FZK 9-179
71

U S A F

NUCLEAR AEROSPACE RESEARCH FACILITY

1 FEBRUARY 1963

(6) FIRST OPERATIONAL YEAR OF THE RTA

(7) NA
(8) NA
(9) NA
(11) 1 Feb 63
(12) 103P-
(13) NA

(10) by

J. T. PANCOAST and
E. L. JORDAN,

(15) CONTRACT
AF 33(657)-7201
11

SECTION II
TASK I, ITEM 6
TASK II, ITEMS 3, 4, 8, and 10
TASK III, ITEMS 2, 3, and 6
OF FZM-2386A

(16) NA
(17) NA
(18-19) NA
(20) U
(21) NA

ISSUED BY THE
ENGINEERING
DEPARTMENT

GD

GENERAL DYNAMICS | FORT WORTH

ACKNOWLEDGMENT

The authors wish to thank the members of the General Dynamics/Fort Worth Reactor Operations Group for their assistance and continued interest in the performance of the RTA experiments.

The authors would like especially to thank Mr. D. F. Ross, who was primarily responsible for the data and presentation of Sections 3.6 and 4.4.

ABSTRACT

On 24 January 1961 the Reactivity Test Assembly (RTA) - a heterogeneous, light-water, unpressurized, fully enriched system that operates as a zero-power reactor - at General Dynamics/Fort Worth was brought critical for the first time. During the year following, the RTA was used in 11 major experiments that covered the operational testing and continued research for the two 3-Mw reactors at the Nuclear Aerospace Research Facility at GD/FW.

REPORT SUMMARY

The Reactivity Test Assembly was constructed to fulfill the need for reactor core data for both operating reactors (GTR and ASTR) at the GD/FW Nuclear Aerospace Research Facility. The use of the RTA in providing these data has minimized NARF reactor operations for parametric data.

GTR Experiments

A series of seven experiments was performed with the 5-rod 3-Mw Ground Test Reactor core configuration. Each of the experiments was performed either to satisfy an immediate requirement for data for proposed experiments or to test and qualify fuel or rods for use in 3-Mw GTR.

The core critical experiment and loading adjustment verified the 35 elements in the final loading so that they might be utilized in the 3-Mw GTR.

The rod calibration was performed to establish the worth of the five control rods.

Fuel-element verification is a recurring experiment performed initially as a monitor on the fuel content and annually thereafter in compliance with Air Force Special-Source Accountability. Verification was performed by comparison of reactivity contribution of unknown elements in a standard core position.

The void reactivity and flux were performed to assess the feasibility and safety of proposed in-pile or in-reflector irradiation positions. These results indicate no apparent hazard increase in the in-core irradiations except those associated with the test specimen.

The fission-plate reactivity contribution was evaluated to determine the limits of perturbation afforded by a U-235 source plate in various configurations.

A control-rod experiment was performed in the interest of providing a replacement rod for the present B_4C rod in use.

Interest in providing a fast-fission source outside the GTR necessitated reactivity measurement of this configuration in a flooded condition.

ASTR Experiments

A series of four experiments was performed with the 3-rod 3-Mw Aerospace Systems Test Reactor core configuration.

The critical experiment was performed with new elements to verify the fuel content of the elements for use in the ASTR Aerospace Systems Test Reactor.

The rod calibration was performed to determine the worth of three new ASTR rods.

The experiment using four rods and a void can was a mockup of a proposed configuration of the ASTR designed to increase the leakage flux from one reactor face and increase the core reactivity.

The neutron-flux distribution in the ASTR core was measured to provide information concerning percentage power contribution of each element and radial anomalies of neutron flux within individual locations.

TABLE OF CONTENTS

	<u>Page</u>
ABSTRACT	3
LIST OF FIGURES	9
LIST OF TABLES	11
I. INTRODUCTION	13
II. EXPERIMENTS USING THE RTA	19
2.1 GTR Experiments	19
2.2 ASTR Experiments	21
III. GTR EXPERIMENTS	23
3.1 GTR-Core Critical Experiment and Loading Adjustment	23
3.1.1 Experimental Equipment	23
3.1.2 Procedure	23
3.1.3 Conclusion	30
3.2 GTR Rod Calibration	31
3.2.1 Experimental Equipment	31
3.2.2 Procedure	31
3.2.3 Conclusion	32
3.3 Fuel-Element Verification	36
3.3.1 Experimental Equipment	36
3.3.2 Procedure	36
3.3.3 Conclusion	38
3.4 Void Measurements	39
3.4.1 Experimental Equipment	39
3.4.2 Procedure	39
3.4.3 Conclusion	44
3.5 Fission-Plate Reactivity Contribution	45
3.5.1 Experimental Equipment	45
3.5.2 Procedure	45
3.5.3 Conclusion	48

TABLE OF CONTENTS (cont'd)

	<u>Page</u>
3.6 GTR Control-Rod Development	49
3.6.1 Experimental Equipment	49
3.6.2 Procedure	49
3.6.3 Conclusions	52
3.7 Moderated-Fast-Section Reactivity Measurement	60
3.7.1 Experimental Equipment	60
3.7.2 Procedure	60
3.7.3 Conclusion	62
IV. ASTR EXPERIMENTS	65
4.1 ASTR-Core Critical Experiment and Loading Adjustment	65
4.1.1 Experimental Equipment	65
4.1.2 Procedure	65
4.1.3 Conclusion	70
4.2 ASTR Rod Calibration	71
4.2.1 Experimental Equipment	71
4.2.2 Procedure	71
4.2.3 Conclusion	72
4.3 Four-Rod ASTR and Void Configuration	72
4.3.1 Experimental Equipment	72
4.3.2 Procedure	75
4.3.3 Conclusion	77
4.4 ASTR-Core Thermal-Neutron Flux Measurements	79
4.4.1 Experimental Equipment	79
4.4.2 Procedure	79
4.4.3 Conclusion	83
REFERENCES	101
DISTRIBUTION	103

LIST OF FIGURES

<u>Figure</u>		<u>Page</u>
1	Reactivity Test Assembly	14
2	RTA Instrumentation and Control	15
3	RTA Tank Interior	16
4	GTR Critical-Experiment Loading Sequence	24
5	Channel 1 Reciprocal Multiplication Curve	26
6	Channel 1A Reciprocal Multiplication Curve	27
7	Channel 2 Reciprocal Multiplication Curve	28
8	Channels 1A and 2 Loading-Adjustment Reciprocal Multiplication Curve	29
9	Shim and Dynamic-Rod Calibration	33
10	Shim and Safety-Rod Calibration	34
11	Reactivity vs Fuel Loading (U^{235})	37
12	Fuel-Element Void Columns	40
13	GTR Void-Reactivity Data	42
14	Void Worth as a Function of Core Location	43
15	Fission-Plate and Positioning Assembly	46
16	Fission-Plate Reactivity Contribution vs Distance from Core	47
17	GTR Core with RTA Lattice Locations	50
18	Cross Sections of Test-Rod Components	51
19	Rod Calibration Curve for GTR Test Rod HA-C-X	54
20	Rod Calibration Curve for GTR Rest Rod HA-C'-X	55
21	Fission-Chamber Traverse in Control Rod Element	56
22	Fission-Chamber Traverse in Control Rod: HA-C-X 12 in. Out	57
23	Rod Calibration of H-C'-X in GTR	59

LIST OF FIGURES (cont'd)

<u>Figure</u>		<u>Page</u>
24	Core Geometry for Flooded Fast-Section Measurements	61
25	Reactivity vs Distance between GTR and Flooded Fast Section	63
26	ASTR Critical-Experiment Loading Sequence	66
27	ASTR Rods-In Reciprocal Multiplication Curves	67
28	ASTR Rods-Out Reciprocal Multiplication Curves	68
29	Safety- and Dynamic-Rod Calibration	73
30	ASTR Reflector Void	74
31	ASTR Control-Rod and Void Configurations	76
32	Flux Measurements in ASTR Void	78
33	Foil-Position Code on Fuel Element	80
34	ASTR Lattice Diagram with Symmetry Assumptions	82
35	Flux Profile across O-Row at Midplane	95
36	Flux Profile across 4-Row at Midplane	96
37	Flux Profile across P-Row at Midplane	97
38	Axial Flux Profile for Lattice Location O-4	98

LIST OF TABLES

<u>Table</u>		<u>Page</u>
I	Poison-Strip Locations	35
II	Reactivity Contribution for Assorted Elements in Grid Position D-3	38
III	Flux Measurements in Void Can	41
IV	Fission-Plate Reactivity Values	48
V	Test-Rod Worth	53
VI	Control-Rod Drop Times	58
VII	Reactivity Contribution of Flooded Fast Section	64
VIII	Power General as Determined by Standard Method	84
IX	Relative Copper-Wire Activities	85
X	Neutron Flux Measurements in Lattice Locations	87
XI	Power Generation by Refined Method	93
XII	Axial Flux Profile for Lattice Location O-4	94

I. INTRODUCTION

General Dynamics/Fort Worth has designed and constructed a flexible critical facility, the Reactivity Test Assembly (RTA). It was constructed to fulfill the need for reactor core data for both operating reactors at the Nuclear Aerospace Research Facility (NARF). The use of the RTA in providing these data has minimized NARF reactor operations for parametric data and thus permitted full-time experimental use of the NARF reactors.

The RTA is a heterogeneous, light-water-moderated, fully enriched, extremely low-power reactor (< 1 kw) capable of adapting to a wide range of core configuration. It is located in Building 144 at the GD/FW facility.

The critical facility vessel, shown in Figure 1, consists of a below-grade 40-inch-diameter, 100-inch-deep aluminum tank with a grid plate capable of accepting a 9×9 array (with the corners missing) of plate-type (MTR) fuel elements. A sump tank of similar volume capacity lies directly beneath the core tank to receive the moderator water during core modifications. A mechanical dump valve in the core tank permits rapid draining for safety shutdowns. For operation, a pump transfers the water from the sump tank to the core tank.

The instrumentation and controls, shown in Figure 2, are monitored and operated from a room adjacent to the reactor room. The core instrumentation, shown in Figure 3, consists of two BF_3 detectors, two fission chambers, and two compensated ion chambers.

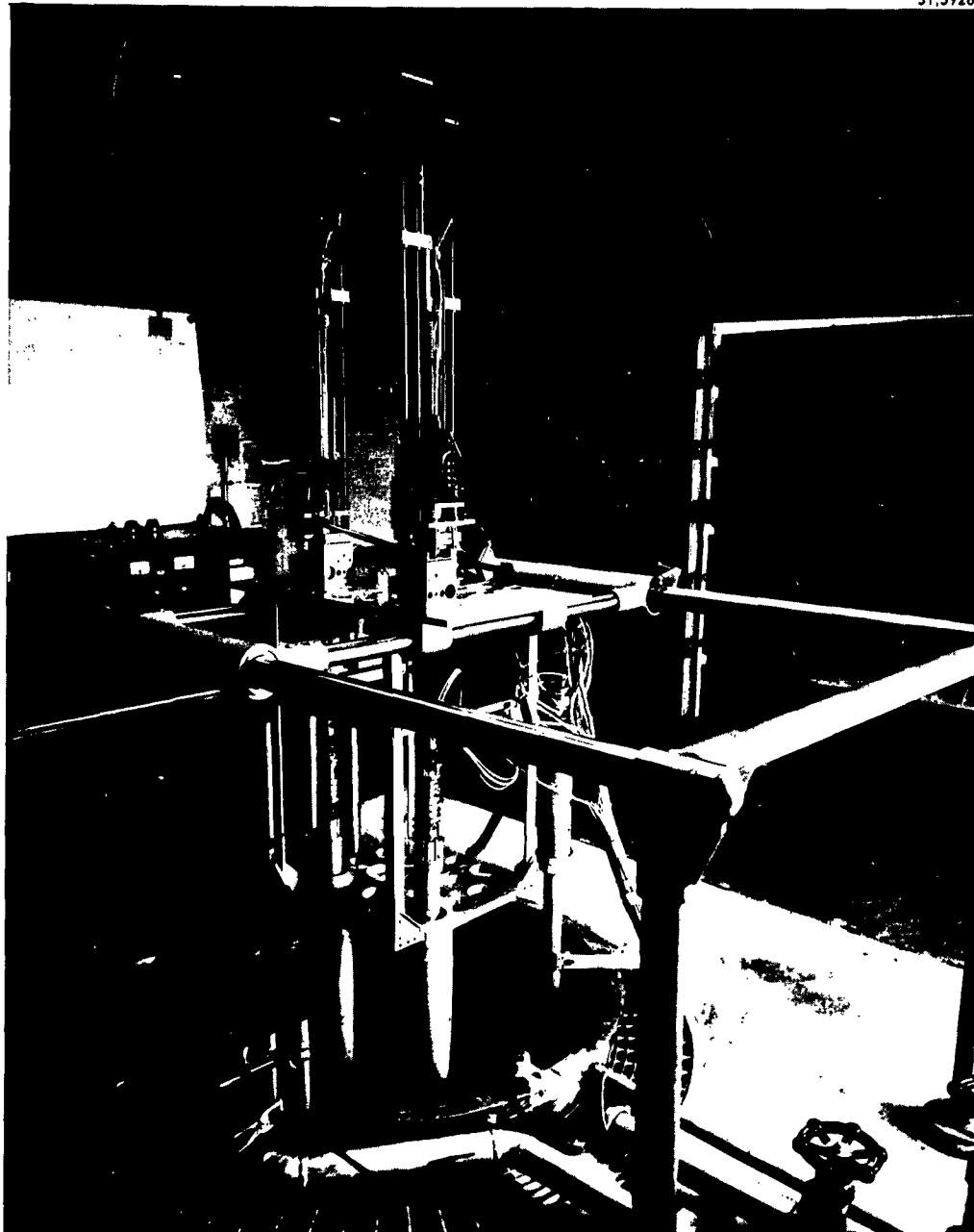


Figure 1. Reactivity Test Assembly

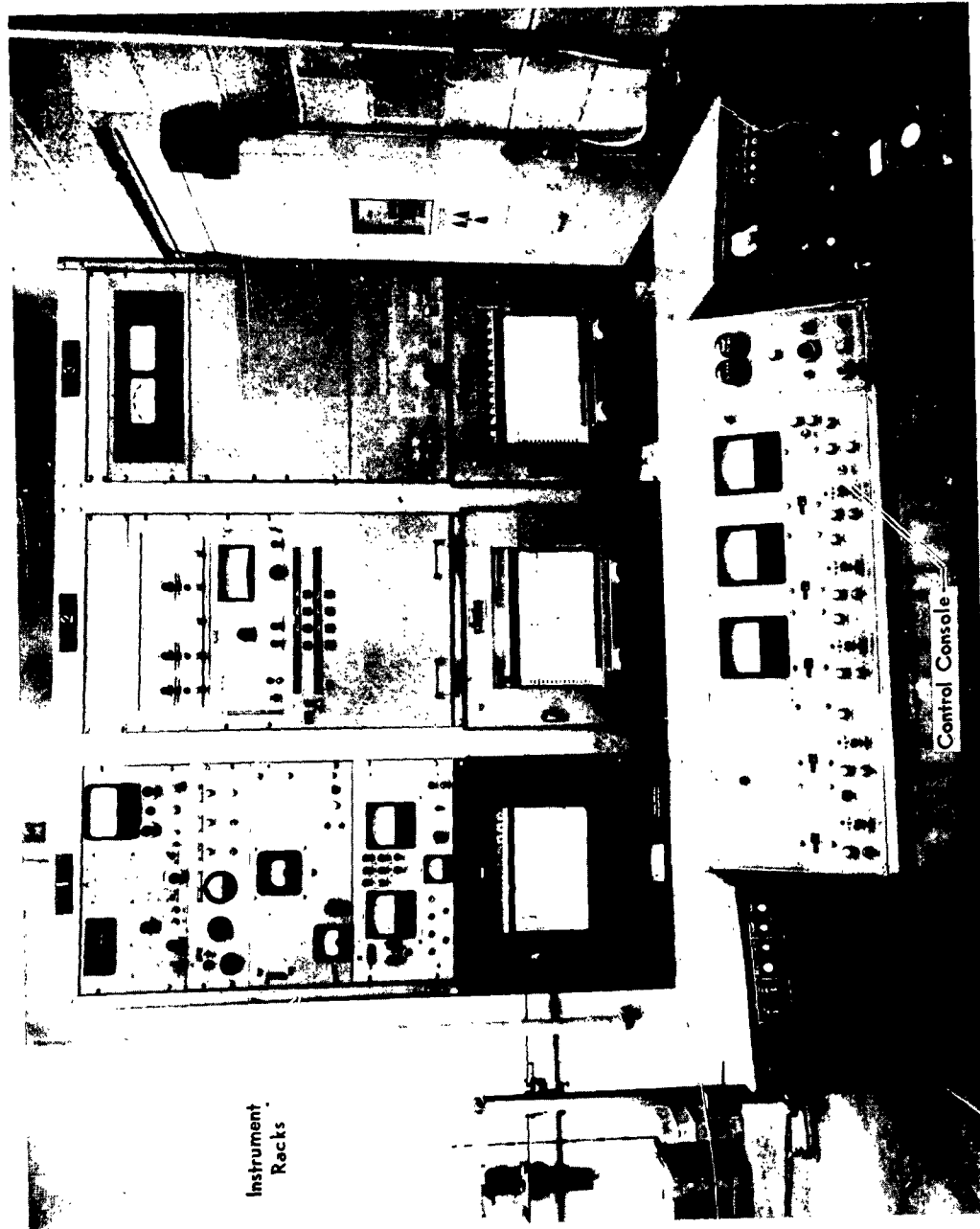


Figure 2. RTA Instrumentation and Control

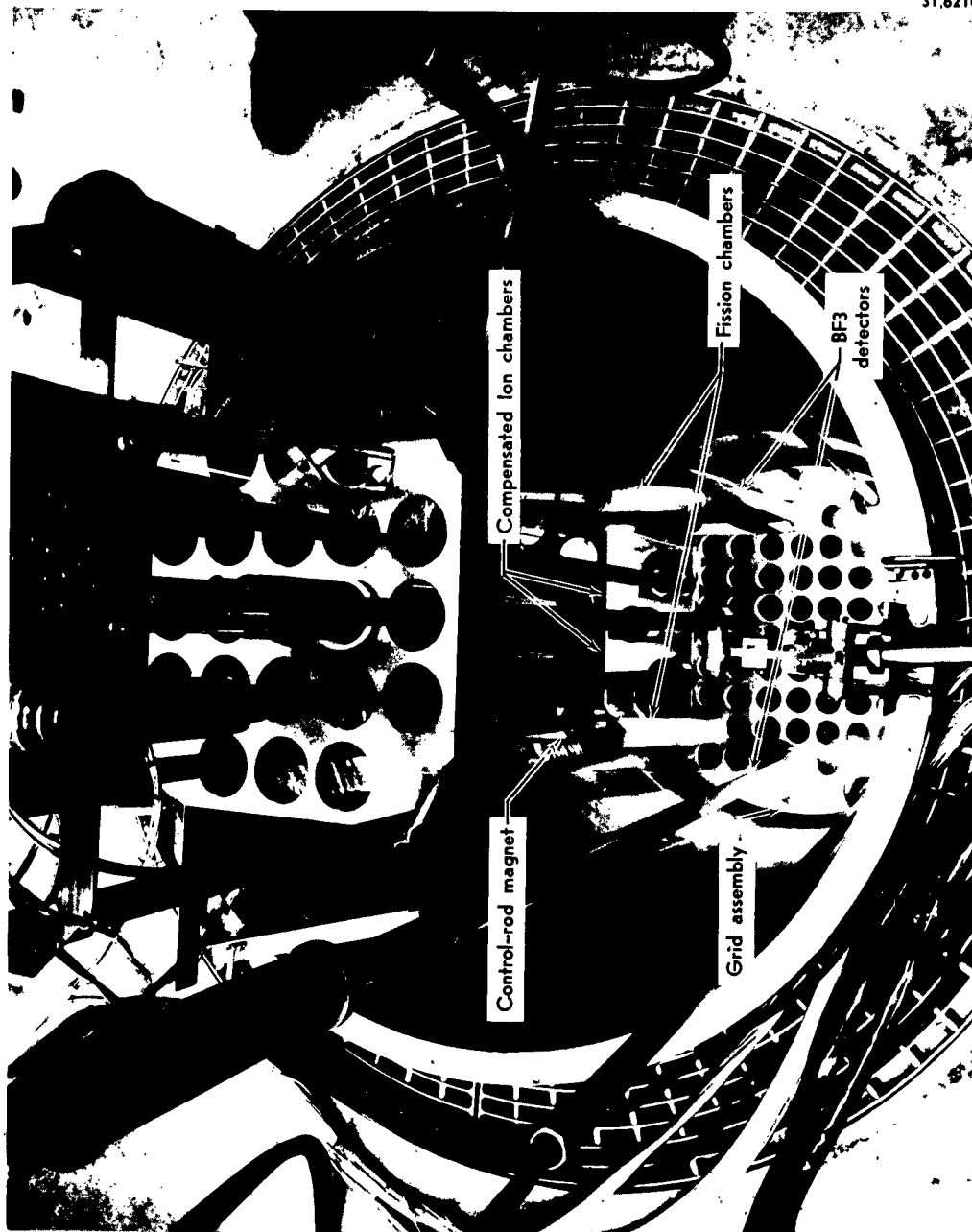


Figure 3. RTA Tank Interior

Five rod drives with electromagnetic couplings provide for the positioning of control rods in the core assembly. In addition, a non-driving electromagnetically coupled safety rod, constructed with a lower fuel section and an upper poison section, is installed near the center of the test configuration. This safety worth is greater than the excess reactivity of the proposed tests.

II. EXPERIMENTS USING THE RTA

2.1 GTR Experiments

A series of seven experiments was performed with the 5-rod 3-Mw Ground Test Reactor (GTR) core configuration in the Reactivity Test Assembly. The experiments consisted of (1) a core critical experiment and loading adjustment, (2) rod calibration, (3) fuel-element verification, (4) void measurements, and (5) source plate measurements, (6) control-rod development and (7) a critical experiment with moderated fast section. Each of the experiments was performed either to satisfy an immediate requirement for data for proposed experiments or to test and qualify fuel or rods for use in the 3-Mw GTR.

The core critical experiment was performed with new elements. In conjunction with the loading adjustment, it verified the 35 elements in the final loading so that they might be utilized in the 3-Mw GTR as a core or portion thereof without a critical experiment.

The rod calibration was performed to establish the worth of the five control rods (conventional design) and the RTA safety element. The rod calibration curves were utilized in subsequent RTA experiments with the GTR core to determine reactivity of the test configurations from critical rod positions.

Fuel-element verification is a recurring experiment performed initially as a monitor on the fuel content as stated by the fabricator and annually thereafter in compliance with Air Force

Special Sources Accountability regulations. Fuel-element content may be verified by either of the following methods:

1. Comparison of critical mass of an assembly of elements with similar assemblies of known elements or with predicted calculated values for a new configuration.
2. Comparison of reactivity contribution of unknown elements in a standard grid position in a known core.

Verification of the fuel elements involved only the second method, inasmuch as the critical experiment and loading adjustment verified the elements of the core assembly by the first method.

The void reactivity and flux determinations were performed to assess the feasibility and safety of proposed in-pile or in-reflector high-flux cryogenic irradiation loops and static samples. The void measurements were performed with fuel-element-equivalent voids placed singularly and in multiples within and on the periphery of the reactor core. Flux measurements were performed for key positions only.

The fission plate reactivity contribution was evaluated to determine the limits of reactivity perturbation afforded by a U^{235} source plate in various configurations with the 3-Mw GTR core and to measure the flux in a void adjacent to the source plate.

A control-rod experiment was performed to establish the limits and preliminary information for further control-rod development. This experiment was performed in the interest of providing a replacement rod for the present B_4C rod in use.

Interest in providing a fast fission source outside the GTR necessitated reactivity measurement of this configuration in a flooded condition. This configuration was mocked up in the RTA and the reactivity contribution from the additional fuel measured as a function of separation between the GTR core and fast section.

2.2 ASTR Experiments

Four experiments were performed with the 3-Mw ASTR configuration in the Reactivity Test Assembly. The experiments consisted of (1) a critical experiment and k_{ex} loading adjustment, (2) a rod calibration, (3) a mockup with a core configuration of four control rods (33 elements) and with a reflector void, and (4) a flux mapping experiment.

The critical experiment was performed with new elements in the 3-Mw ASTR configuration. In conjunction with the loading adjustment, it was intended to verify the fuel content of the elements and to prepare the assembly for use in the ASTR.

The rod calibration was performed to determine from the loading adjustment the incremental worth of three new ASTR rods in the resultant configuration. The curves thus obtained were utilized in subsequent experiments to determine reactivity of test configurations from critical-rod positions.

The core configuration with four rods and a void was an experimental mockup of a proposed configuration of the ASTR designed to increase leakage flux from one reactor face and increase the core activity.

The power distribution in the ASTR core was studied for three reasons. First, the power distribution in the core is a necessary parameter in core heat transfer calculations. Second, the power distribution of the core directly affects the source term that is necessary for all shielding calculations. Third, the power generated can be related to currents from ion chambers, resulting in power calibration of the ion chambers.

Previous study of the ASTR core for these reasons (Refs. 1 and 2) disclosed the need for further work in determining the neutron flux distribution within individual elements.

Three cores have been used in the ASTR. The third and present core was procured from Babcock and Wilcox in May 1961. The construction of these elements differed from the first two cores in that the fuel plates were pinned to the side plates, rather than brazed. Accordingly, it was decided to make a complete survey of the neutron flux distribution in this new core.

The purpose of the experiment was to disclose:

1. Percentage contribution of each location to total reactor power;
2. Vertical maximum-to-average flux ratio of each location; and
3. Presence or absence of radial anomalies of neutron flux within individual locations.

III. GTR EXPERIMENTS

3.1 GTR-Core Critical Experiment and Loading Adjustment

3.1.1 Experimental Equipment

The RTA tank was set up to receive the core components for a 5-rod GTR loading. The instrumentation consisted of normal RTA operation instrumentation (Ref. 3). The location of the detectors and source is shown on Figure 4, Loading 1. The fuel elements used for this critical experiment were 140-gm U^{235} GTR elements. With the exception of the 70-gm control-rod elements, only full elements were used in this experiment.

3.1.2 Procedure

In preparation for loading, the detectors were source-checked, the scram checks were performed, and the water was drained to the sump tank. The first loading consisted of five rod elements and three full elements (Fig. 4, Loading 1).

The loadings were each performed in a dry tank. When the water level was raised, both "rods in" and "rods out" multiplications were obtained. Then the rods were inserted and the water dumped. Subsequent loadings to criticality followed the same procedure. The number of elements to be added in each increment was determined by extrapolation of rods-out multiplication, along with the limitation on each increment of never adding more elements than the preceding increment. The loading sequence to criticality is shown in Figure 4, Loadings 1 through 11.

24

Reciprocal multiplication versus number of fuel elements is shown in Figures 5, 6, and 7 for Detectors 1A and 2. Rods-in and rods-out multiplication curves were compared to show effectiveness of the uncalibrated control rods and thereby further ensure the safety of the experiment. After criticality was established at 25.5 elements (3570 gm U²³⁵), the remaining elements to the full 3-Mw loading of 32.5 elements (4550 gm U²³⁵) were added one element at a time (Fig. 4, Loadings 12-18). The loadings were each performed in a dry tank following the same procedure as before criticality. Rods-in multiplication, shown in Figure 8, was obtained for each loading.

A study of the reciprocal multiplication curves shows that the geometry of source, fuel, and detector may cause large variations in the slope of the curves from one detector to another. The number of elements added at any one increment must be weighted by consideration of geometry of the previous configurations.

Two procedural discrepancies were noted during this experiment. The first involved placement of fuel relative to the source in Step 2 of the loading. The steps as indicated by the planning document required the addition of six elements, two of which were installed in "C" row and which, because of their proximity to the source, acted as a source plate and gave a one-element extrapolated criticality. The loading was modified and only one element was left in row C, allowing two

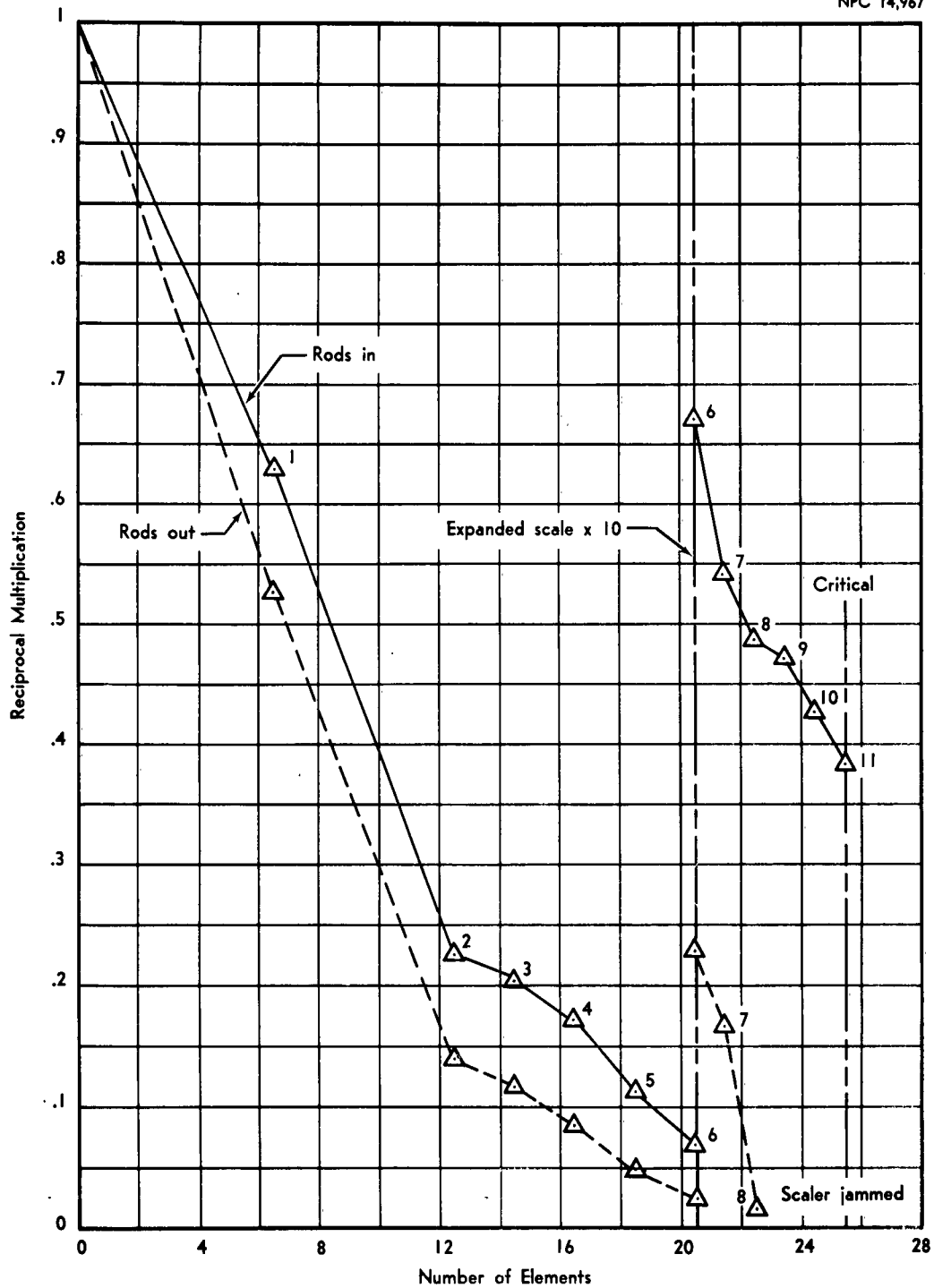


Figure 5. Channel 1 Reciprocal Multiplication Curve

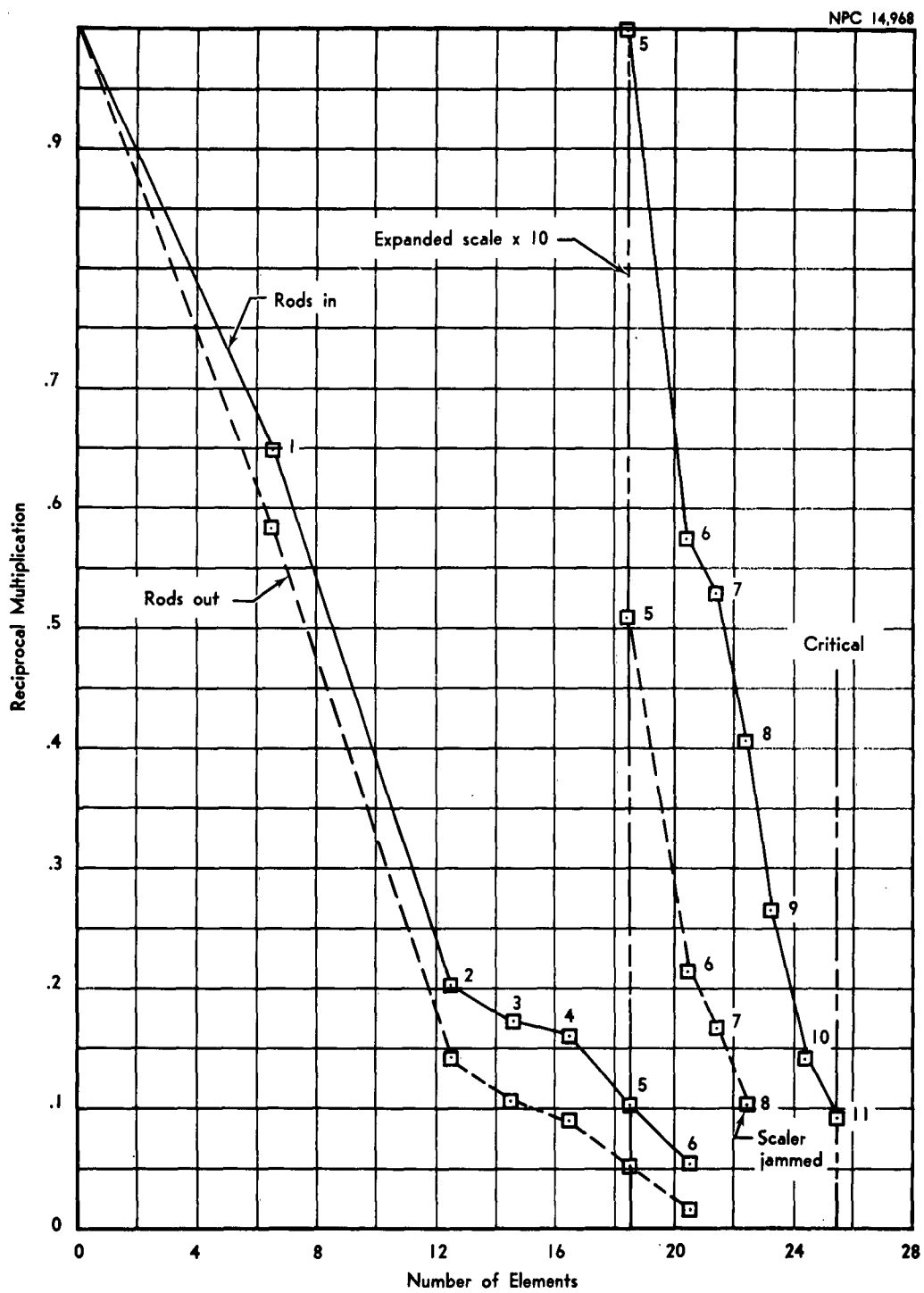


FIGURE 6. Channel 1A Reciprocal Multiplication Curve

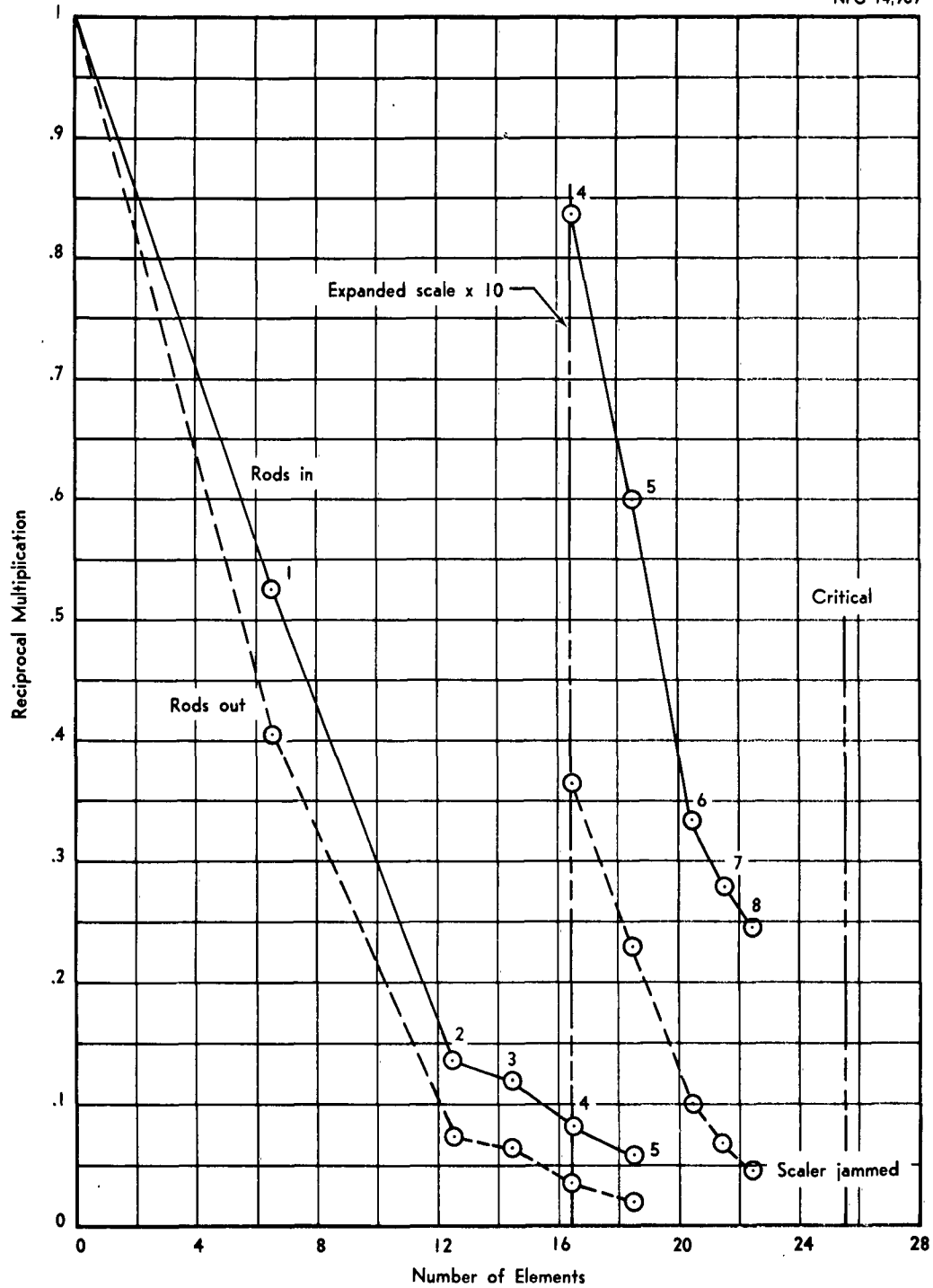


Figure 7. Channel 2 Reciprocal Multiplication Curve

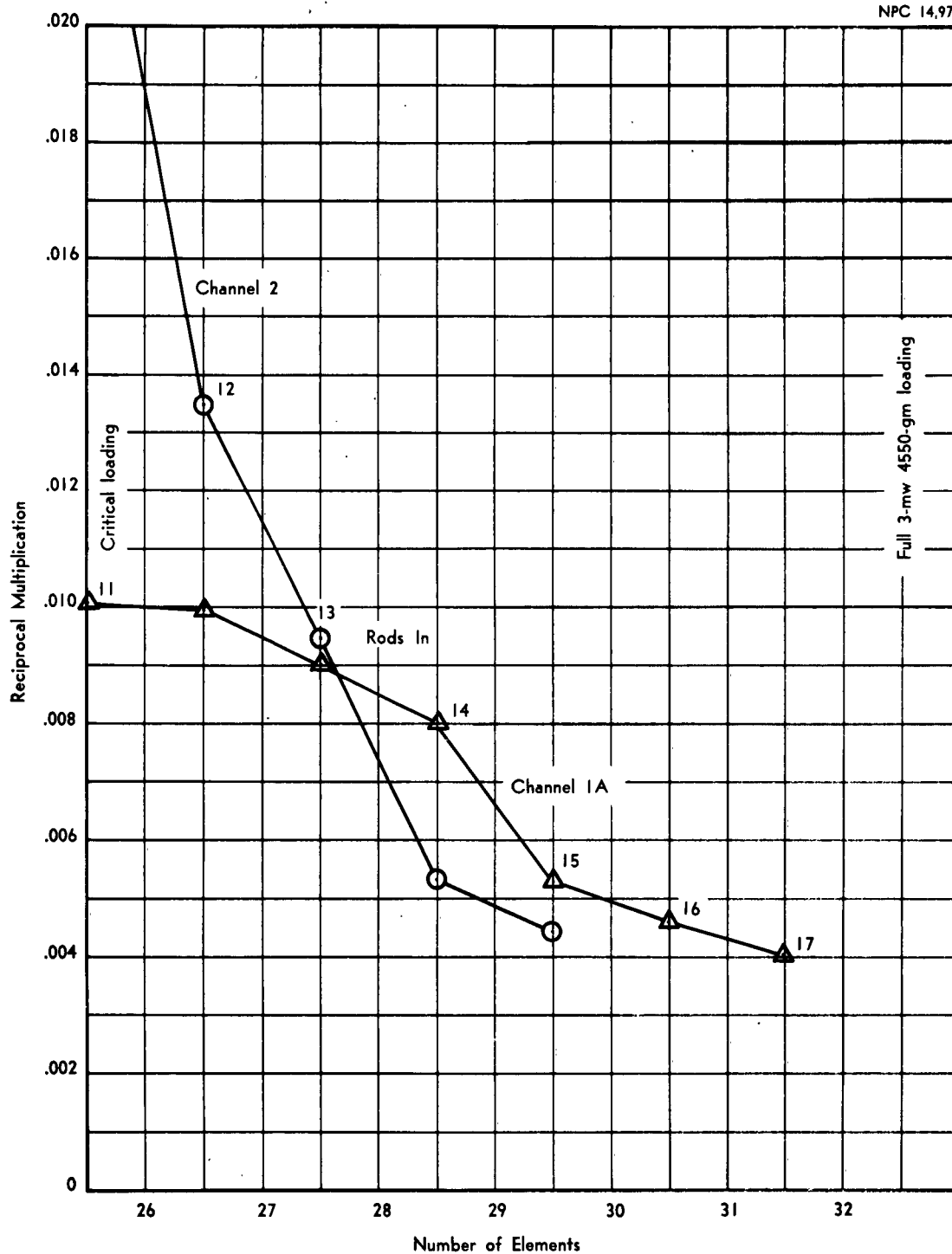


Figure 8. Channels 1A and 2 Loading Adjustment Reciprocal Multiplication Curve

elements to be added in Step 3 (Figure 4). A solution to this problem could lie in (1) multiple sources or (2) a single central source located within the safety element. The source, when not in use, would then be submersed into the safety-element recess.

The second procedural discrepancy resulted from a very high BF_3 count rate when criticality was approached, resulting in jamming of the scalers with rods out. The source count rate for Channels 1, 1A, and 2 was 13,700, 10,700 and 5,200 cps, respectively. Rods-out multiplication of Loading 8 was measured at approximately 500-1000, yielding count rates of the order of a megacycle. The Advance Airborne Dual Scalers in use during this experiment were incapable of accurately counting above 500 kc. Adoption of a Berkley Universal Eput Timer Model 7360 or similar megacycle or better counter for at least one BF_3 channel and desensitizing the BF_3 's at least one decade by a central source and use of a greater separation distance from the core (such as grid positions A-2 and 8) should alleviate this problem.

3.1.3 Conclusion

The RTA was made critical on a 3570-gm, 5-rod, 23-element array at 1:30 a.m., 24 January 1961. This critical configuration was identical to previous GTR cores and, in addition, agreed with calculated criticality, thus indicating the same total fuel content. The reactor at this loading possessed approximately 0.15% $\Delta k/k$. The reactor core adjusted to the operational 3-Mw loading of 4550-gms U^{235} possessed 4.64% $\Delta k/k$ excess reactivity.

3.2 GTR Rod Calibration

3.2.1 Experimental Equipment

The experiment was begun with the loaded 3-Mw GTR core configuration resulting from the critical experiment and loading adjustment. Normal RTA instrumentation was utilized for this experiment (Ref. 3). A total of ten 1/2-in. x 30-in. x 20-mil cadmium strips were used as required to "poison" the core during shim-rod calibration.

3.2.2 Procedure

The five control rods were evaluated by the period method, i.e., correlation of incremental rod travel with the resulting stable period by use of the In-Hour equation. Rod calibration sequence was in the order of use, i.e., dynamic, shim-safety, and shim. The procedure was essentially the same for each rod. The reactor was made critical with the rod to be calibrated fully inserted in the core. The source was removed to permit accurate period measurement at very low power levels. A long period (300-400 sec) was established by withdrawal of one of the rods not being calibrated, and the stable period was measured from the Channel 4 recorder with a stop watch. Then the rod being calibration was withdrawn some small increment (3-in. in the case of dynamic, 1-in. shim safety, and shim) and the resultant stable period again measured. Additional rod increments were measured until the period approached either 7 sec or the power level of 1 kw. Then the other rods were inserted sufficiently to reduce the power to the starting level. At this

point, a long period was again established and the entire procedure repeated until the full length of the rod was calibrated. The reactor was then shut down in preparation for the next rod to be calibrated. The dynamic and shim-safety rods were calibrated in a poisoned-down 4.5% $\Delta k/k$ 3-Mw core by offsetting withdrawal of the rod being calibrated with insertion of another after the period corresponding to each increment of rod worth had been measured. Shim 1 rod was calibrated with the core poisoned down, so that the shim-safety rods were full out. Poison strips were inserted to obtain the initial position and were added as Shim 1 was calibrated (see Table I). The dynamic was utilized to extend the range of shim rod that could be calibrated before repointing. Shim 2 was calibrated with Shim-Safety 1, Shim-Safety 2, and Shim 1 full out. Rod worth % $\Delta k/k$ versus inches withdrawn are shown in Figures 9 and 10.

The safety-element value was estimated at approximately 10% $\Delta k/k$ by withdrawing all control rods while the safety remained inserted and observing multiplication along with knowledge of excess reactivity in core and rod values.

3.2.3 Conclusion

It is known that rod values obtained in the manner described are not absolute and that they change with burnup and buildup of stable poisons in an operating reactor. A comparison with identically constructed rods as used in the operating GTR show total-rod-worth agreement of $\pm 7\%$. Rod worths as determined

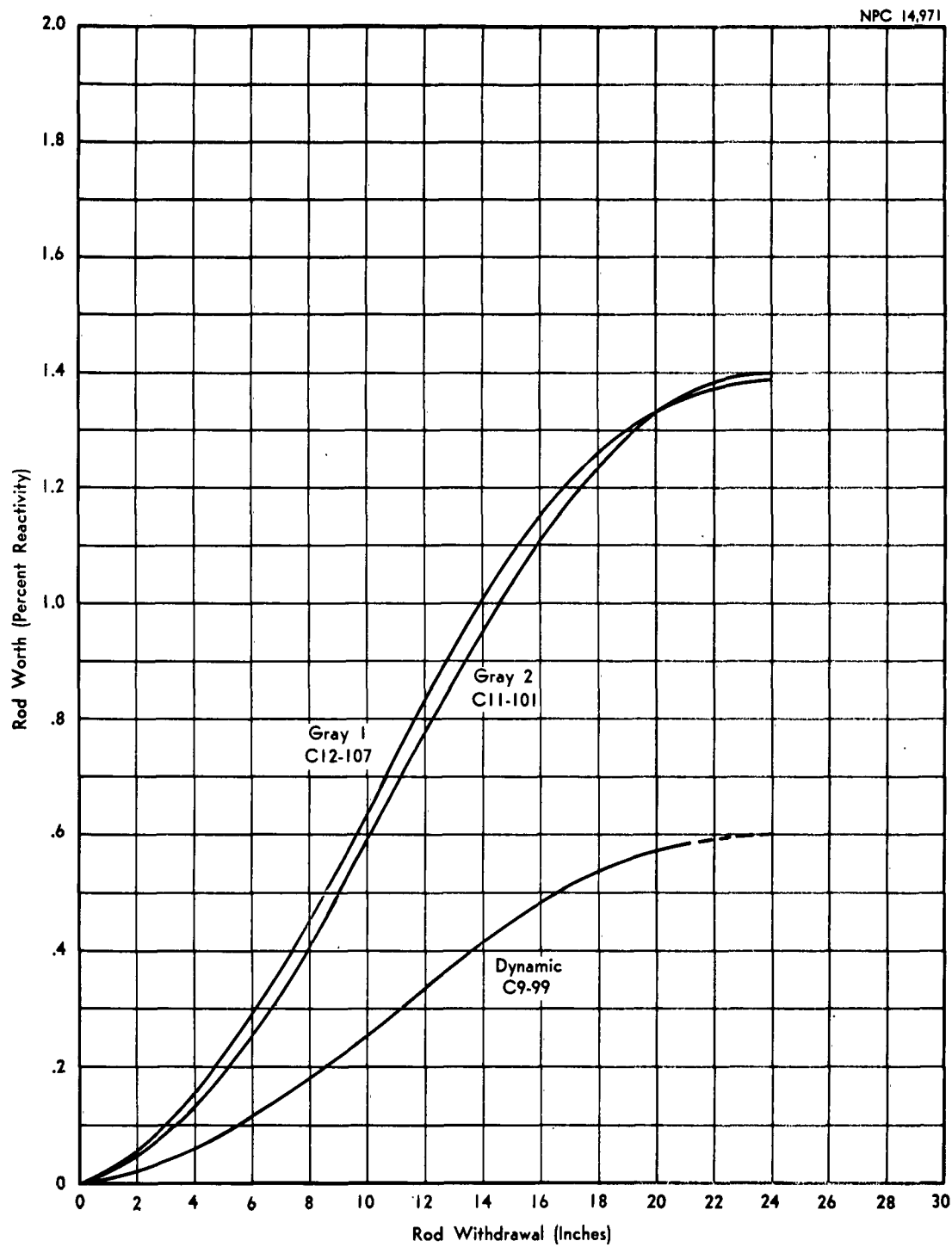


Figure 9. Shim and Dynamic-Rod Calibration

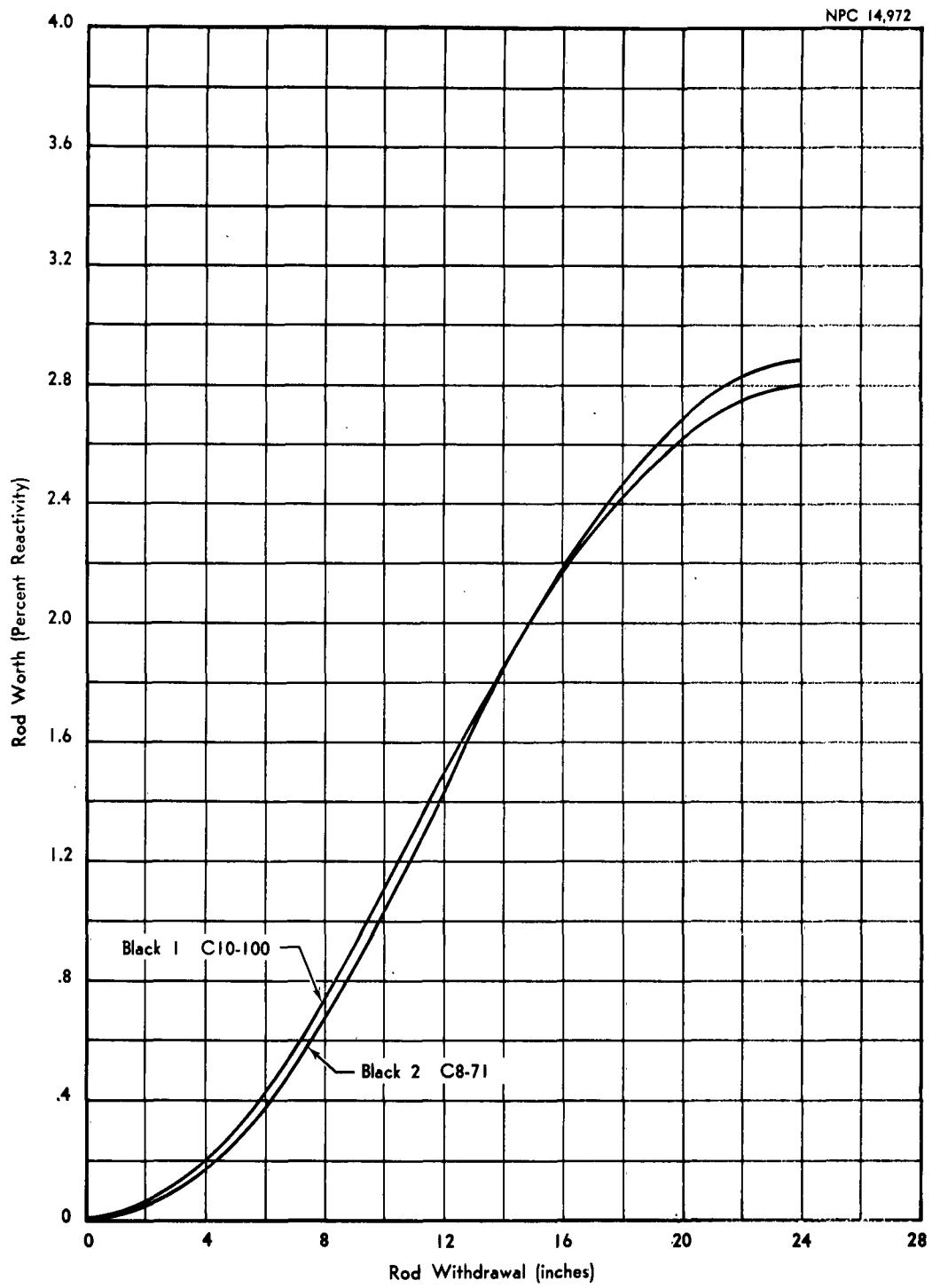


Figure 10. Shim-Safety-Rod Calibration

in the RTA are consistently higher than those determined in the GTR, indicating that the difference is due to the change in the manner of calibration. The GTR rods were calibrated as reactivity became available during xenon decay following a long 3-Mw run.

TABLE I
POISON-STRIP LOCATION

Rod	Increment (in.)	Location of Cadmium Poison Strips	Reactivity Worth (%)
G-1	0- 9	E-2, F-3, D-7, E-7, F 7 (6-in. withdrawn)	-1.86
G-1	9-14	as above F-7 full in plus D-3	-2.30
G-1	14-23.6	as above plus C-3, G-3, C-7	-2.85
G-2	0-10	E-2, F-3, G-3, D-7, E-7 F-7, D-4, D-6, D-3 (6-in. withdrawn)	-3.25
G-2	10-15	as above D-3 full in plus C-3, C-6	-3.65
G-2	15-24.48	D-3, E 3, F-3, D-4 (2 strips), D-6 (2 strips), D-7, E-7, F-7	-4.14

3.3 Fuel-Element Verification

3.3.1 Experimental Equipment

The experiment was begun with the loaded 3-Mw GTR core configuration. Normal RTA instrumentation (Ref. 3) was utilized during the experiment.

3.3.2 Procedure

The excess reactivity was observed for the standard 4550-gm 3-Mw GTR loading, the tank was drained, and the element in grid position D-3 was replaced by the element to be verified. The safety element was cocked and the tank filled. Then the reactor was brought to power at one nominal watt, with rod positions being observed after source removal. The reactor was shut down, the tank drained, and the source reinserted. Dummy and progressive increments of partial elements to full 140- and 150-gm elements were cycled through grid position D-3 of the known 3-Mw GTR core. This procedure was repeated for each element being verified. As shown in Figure 11, reactivity contribution for each element versus fuel content (gm U²³⁵) as stated by the fuel fabricator was plotted. The reactivity varied from zero contribution for the dummy to 1.8% for a 150-gm ASTR element. Reactivity contribution was determined from critical rod positions at one nominal watt with the source removed (Table II).

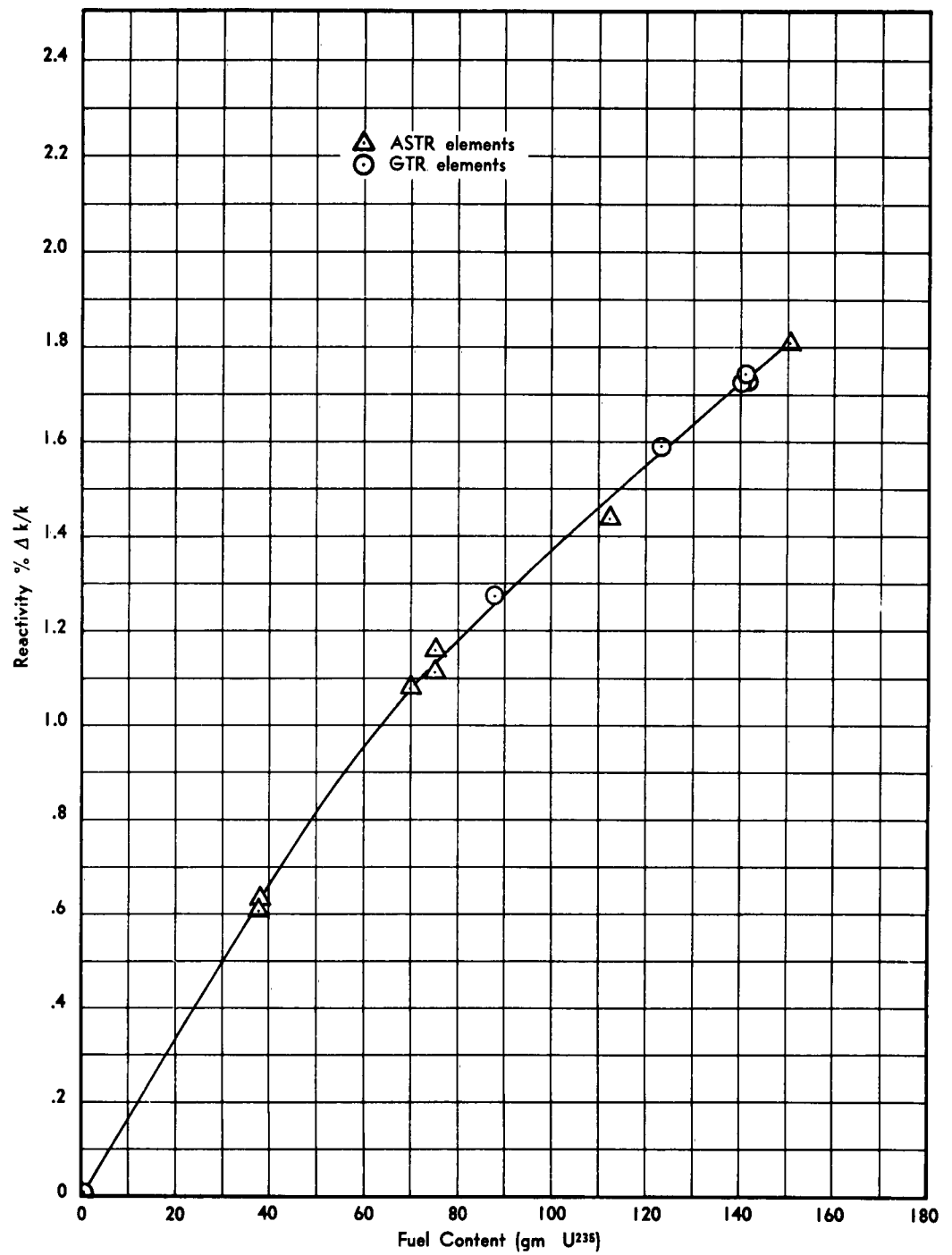


Figure 11. Reactivity vs Fuel Loading (U^{235})

TABLE II
REACTIVITY CONTRIBUTION FOR ASSORTED ELEMENTS
IN GRID POSITION D-3

Fuel Element Number	Fuel Content gram U235 (fabrication)	Reactivity Contribution
Dummy	0	0
ASTR CD-35	37.52	0.637
GTR P-8-104	70.06	1.078
ASTR CC-37	75.03	1.115
GTR P-7-103	87.60	1.267
ASTR CB-39	112.37	1.432
GTR P-6-102	123.13	1.574
GTR S-92	139.99	1.718
ASTR AC 45	151.08	1.808
ASTR CC-38	74.98	1.103
GTR S-91	141.13	1.722
GTR S-90	141.14	1.735
ASTR CD-36	37.52	.619

3.3.3 Conclusion

The collected data are insufficient for a conclusive statistical analysis of permissible deviations. The variation in data may be a result of inaccuracies in rod calibration (used to ascertain reactivity effect from rod position) and/or change of rod worths as a result of perturbation of reactor flux due to the the "test" element in the "standard" position. The threshold of

detection of variation of fuel content as ascertained from these data appears to be less than +3%.

3.4 Void Measurements

3.4.1 Experimental Equipment

The 3-Mw GTR core configuration and normal RTA instrumentation were used with the ASTR reflector void and two fuel-element voids to comprise the experimental equipment.

The ASTR void is described in Section 4.3.1 and Figure 30. The fuel element voids were constructed from extruded square tube with 0.10-inch walls and welded on top and bottom to form a 3- by 3- by 24-in. tall vessel equivalent to the maximum useful volume available for in-core irradiation tests by substitution for a fuel element (Fig. 12). The fuel-element voids were ballasted and provided with pressurization similar to the ASTR voids. The fuel-element voids were pressure-checked to 120 psi and operated at 10 psi as a result of the predicted large void worth.

3.4.2 Procedure

Criticality was checked for the 3-Mw GTR configuration resulting from the critical experiment discussed in Section 3.1. The reactivity observed from critical rod positions served as the base measurement from which the effects of the voids in the various locations were determined.

The initial measurements established the reactivity change resulting from a void collapse and removal from RTA grid position D-3 as -0.13% and -0.20% $\Delta k/k$, respectively. This measurement was performed to determine the maximum possible reactivity change that

NPC 14,974
31,6211

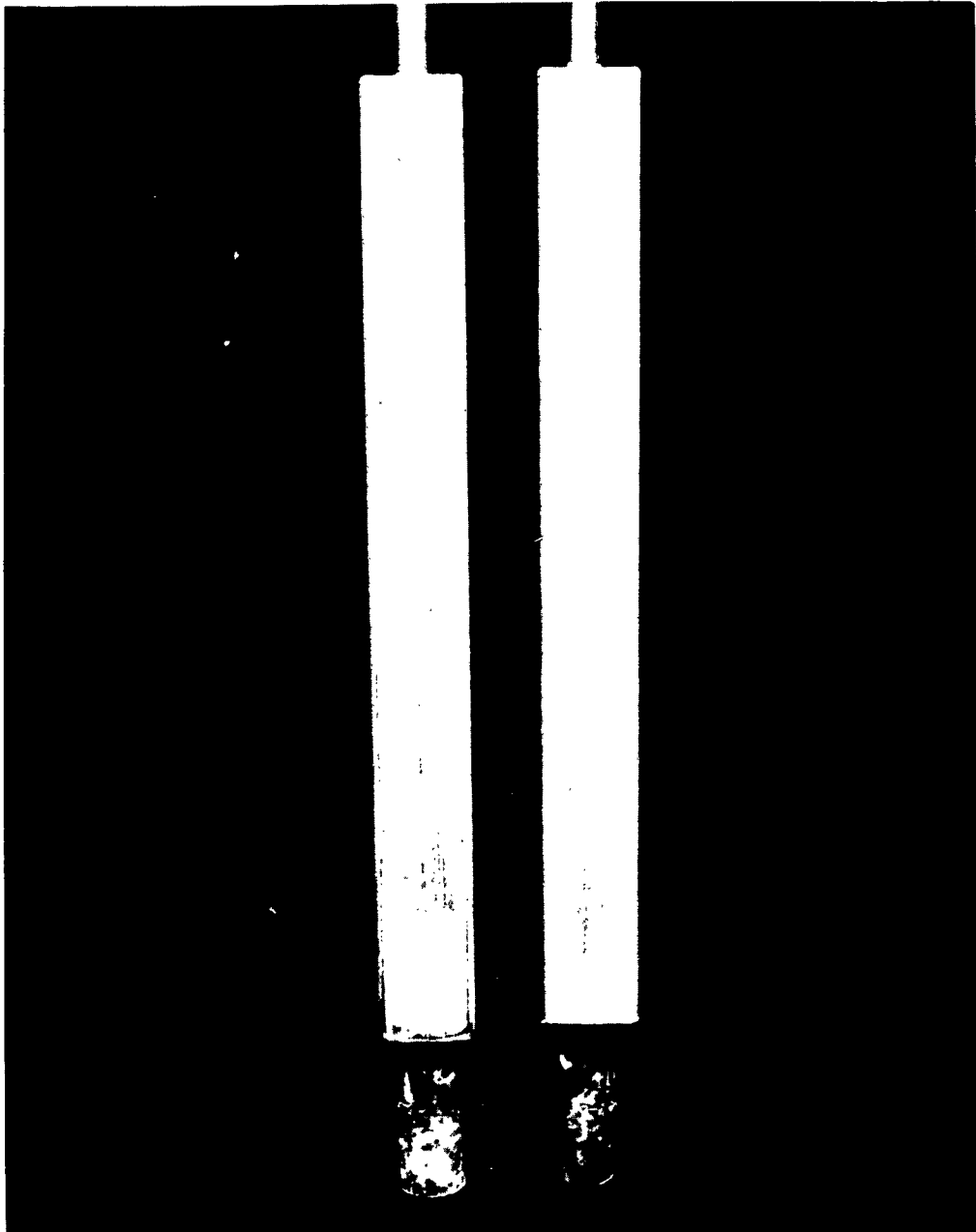


Figure 12. Fuel-Element Void Volumes

could occur. The data show a loss rather than a gain in reactivity; hence, no harmful effects could result.

The single-element void was placed in RTA grid positions C-3, D-3, E-3, F-3, C-2, C-3, C-4, C-6, C-7, and C-8 and the reactivity effect measured. G-4 was omitted because of the symmetry observed between C-3, E-3. The two void cans were installed in C-2 and C-3 and then in C-2 and D-2. The internal reactivity effects are shown in Figures 13 and 14.

Thermal-neutron flux measurements were obtained by exposing bare and cadmium-covered gold foils in the center of the void can for internal positions D-3, C-2, and the two-element void in positions C-2 and C-3. Fast-flux determinations were made by exposing sulfur in a separate run for each of the above positions. The flux data are given as n/cm^2 -sec-watt in Table III.

TABLE III
FLUX MEASUREMENTS IN VOID CAN

Void Location		Flux per Watt	
RTA	GTR	n_{th}/cm^2 -sec-watt	n_f/cm^2 -sec-watt
D-3	D-6	6.8×10^6	4.6×10^5
C-2	E-7	6.0×10^6	7.5×10^5
C-2*	E-7	5.4×10^6	5.7×10^5
C-3*	E-6	6.0×10^6	1.4×10^6

* The two-element void volume

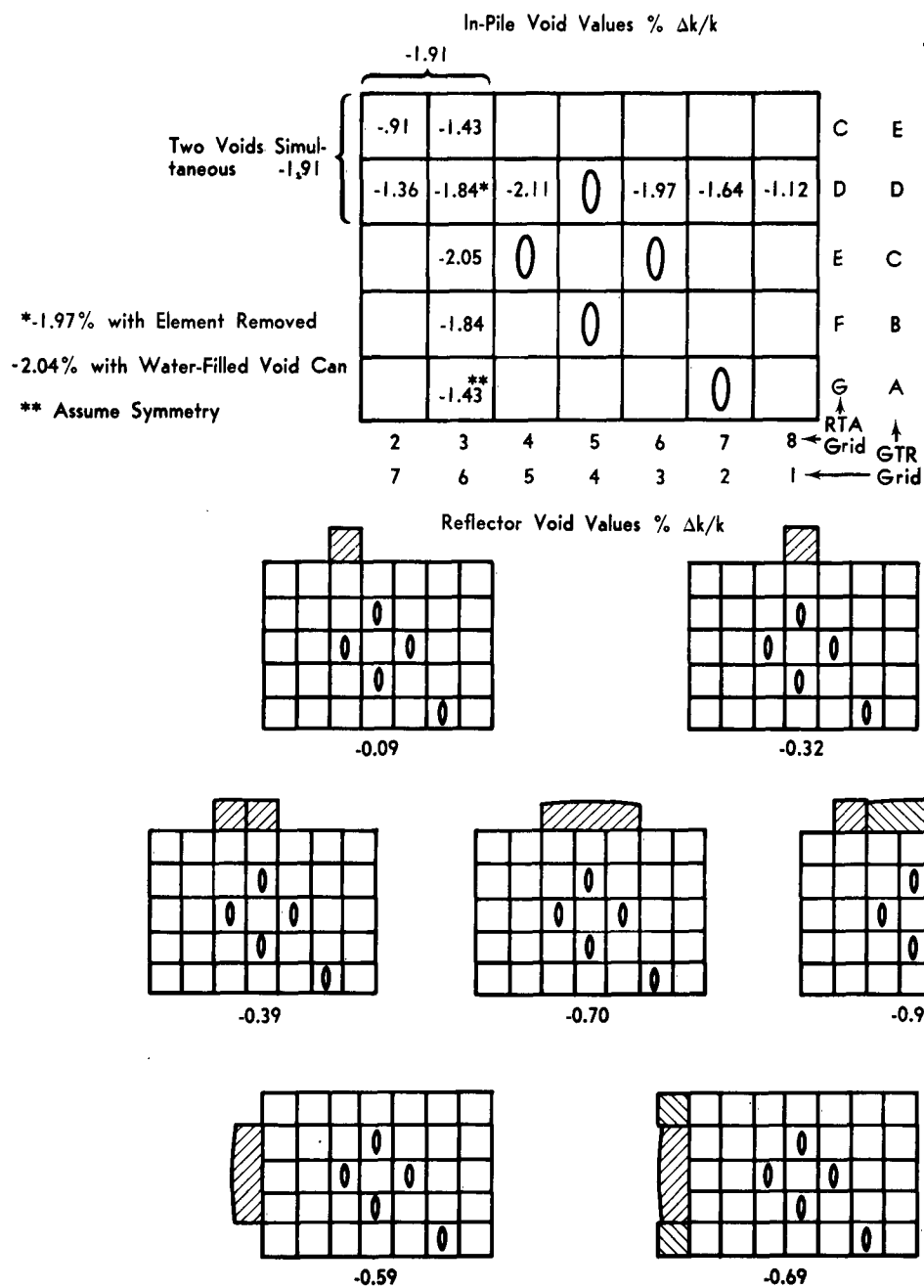


Figure 13. GTR Void-Reactivity Data

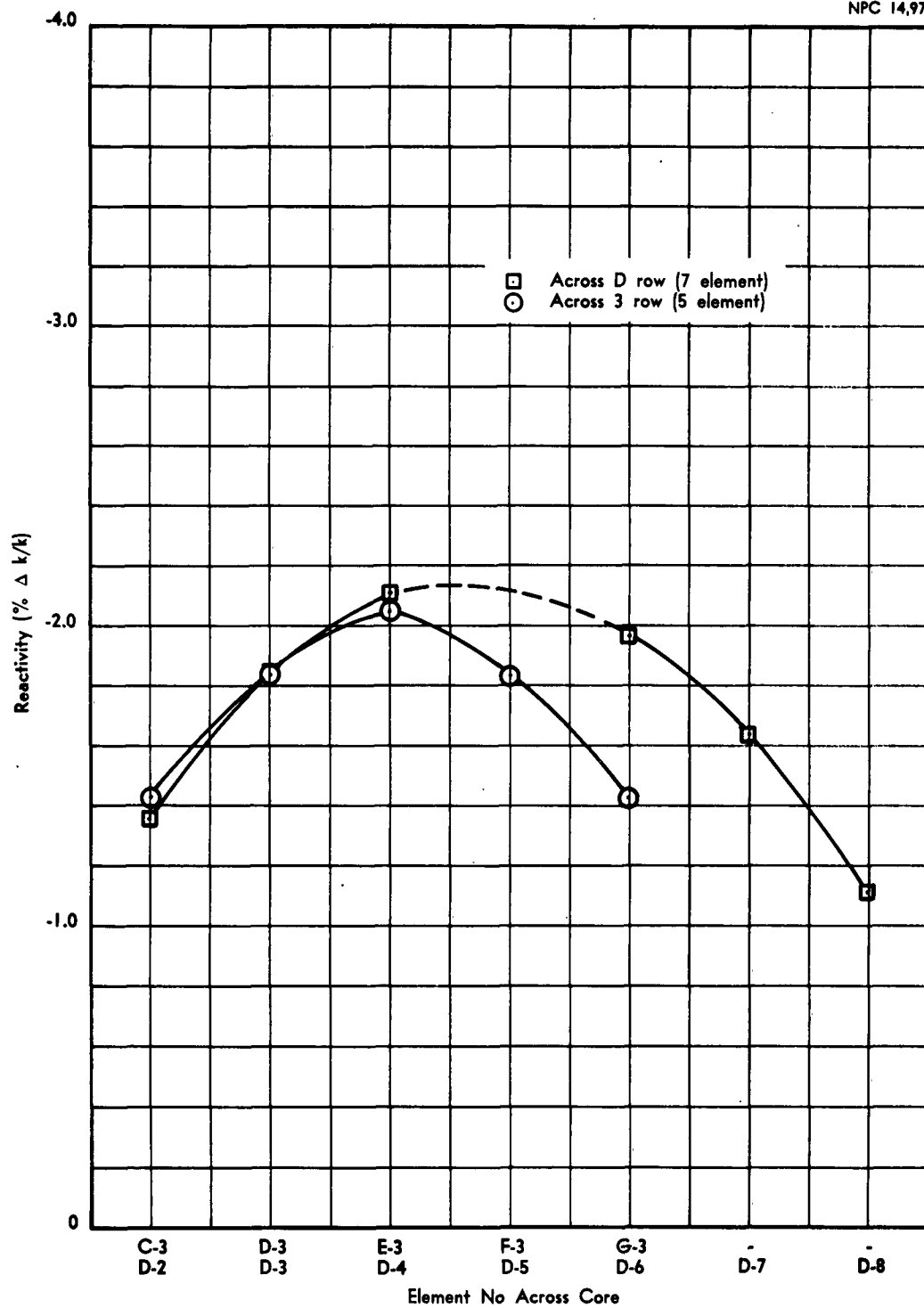


Figure 14. Void Worth as a Function of Core Location

Reactivity effects resulting from placing the void cans adjacent to a core face singly and then in multiples were determined for the seven-element front face and a five-element side. These values are shown in Figure 13.

3.4.3 Conclusions

In-core irradiations with the GTR could be performed with no increase in the apparent hazard except those resulting from perturbations due to a test specimen. Complete flooding of the void container or removal of the container from the core would result in a loss of reactivity. The maximum thermal-neutron flux in a void 3- by 3- by 24-in. container in GTR position D-6 (RTA D-3) at 3 Mw should be 2×10^{13} n/cm²-sec. An average-to-maximum flux ratio of 0.77 observed in a normal fuel element should still prevail in the sample container. A sample 3- by 3- by 24-in. container in GTR core position E-6 and E-7 (RTA C-2 and C-3) should yield a maximum thermal-neutron flux of from 1.6 to 1.8×10^{13} n/cm²-sec.

Due to the assumptions of the core flux profile made during the flux measurements to determine reactor power, the calculated fluxes are necessarily $\pm 20\%$. More precise data would require a complete core mapping and calibration for each of the flux determinations.

3.5 Fission-Plate Reactivity Contribution

3.5.1 Experimental Equipment

The 3-Mw GTR core configuration with normal startup instrumentation was utilized during the experiment. A 4.5- by 5.5- by 0.5-in. 466-gm U^{235} source plate and holder (Fig. 15), along with the ASTR 9- by 4- by 16-in. void tank (Fig. 30), constituted the additional equipment necessary to perform the experiment.

3.5.2 Procedure

The initial phase of the experiment consisted of measuring the reactivity contribution of the source plate as a function of separation distance from the center of the front face of the reactor core with separation distances of between 0.125 and 6.0 inches (Fig. 16). The reactivity change was obtained from observation of critical rod position and referral to rod calibration curves (Figs. 9 and 10).

The second phase of the experiment utilized data of the initial phase as an upper limit to possible reactivity perturbations. The reactivity effect was determined with the source plate displaced vertically ± 5 inches from the maximum effective position. In addition, the reactivity effect was measured with the source plate resting on the grid plate adjacent to the front face and then resting face down and centered over lattice position D-3 (Table IV).

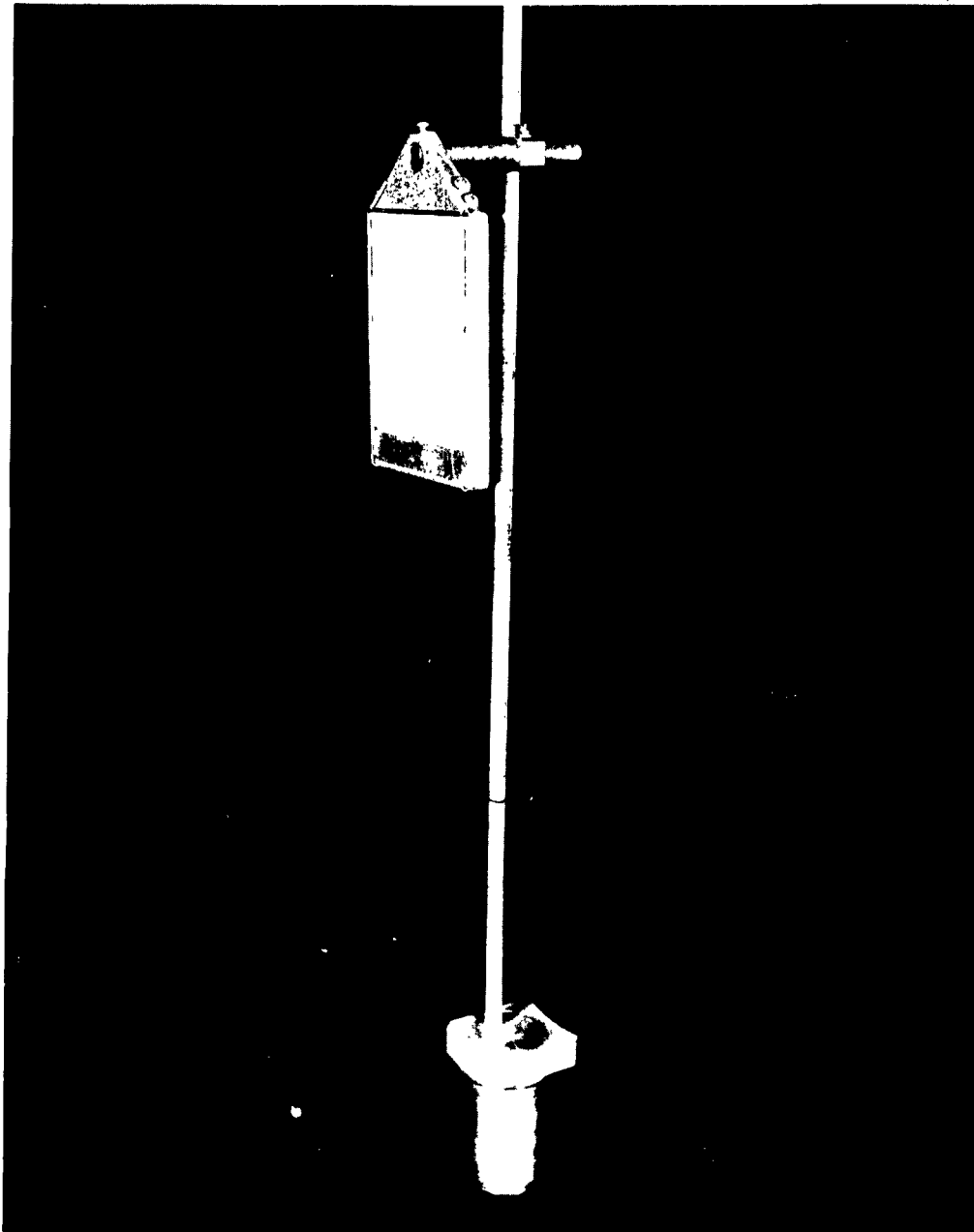


Figure 15. Fission-Plate and Positioning Assembly

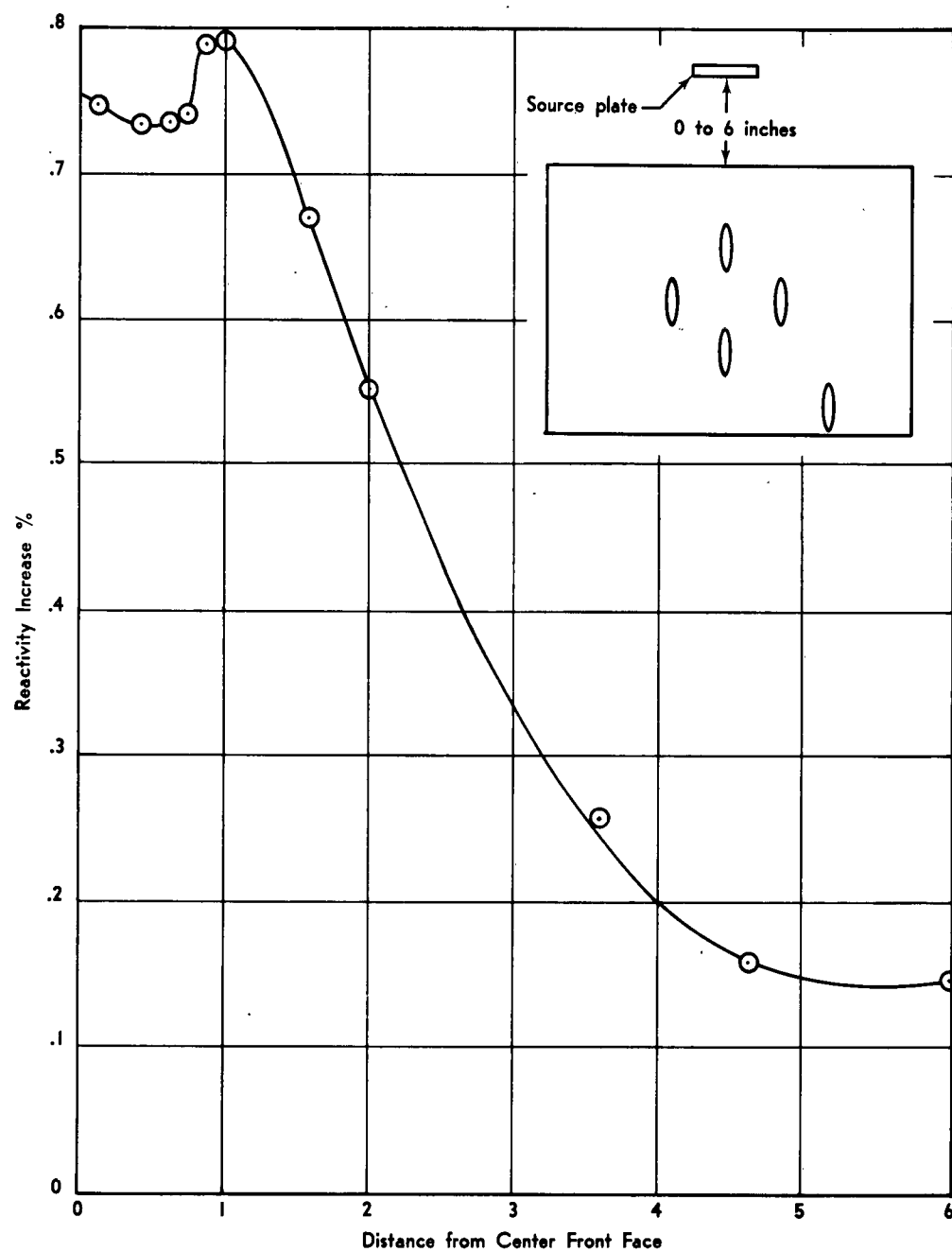


Figure 16. Fission-Plate Reactivity Contribution vs Distance from Core

TABLE IV
FISSION-PLATE REACTIVITY VALUES

Distance from Center Front Face (in.)	Reactivity Contribution (% $\Delta k/k$)
6	0.15
4.625	0.16
3.625	0.26
2.0	0.55
1.625	0.67
1.0	0.794
0.875	0.79
0.750	0.74
0.625	0.735
0.375	0.735
0.125	0.745

3.5.3 Conclusion

The peak reactivity contribution of $+0.79\% \Delta k/k$ was found to occur with the source plate one inch from the center of the reactor front face. An increase in excess reactivity of $0.31\% \Delta k/k$ was observed with the source plate resting over D-3 and an increase of $0.44\% \Delta k/k$ when it is allowed to rest upright on the grid plate adjacent to the core. The latter two measurements were devised to show the maximum reactivity perturbation resulting from the source plate coming to rest on the core or on the grid plate of the 3-Mw GTR. Normal reactor instrumentation could effectively handle an increase of this magnitude without endangering operating personnel or the reactor.

3.6 GTR Control-Rod Development

3.6.1 Experimental Equipment

The standard GTR loading of a 5 x 7 lattice was used during this experiment. Black-rod location (RTA grid position E-4) was used in all cases as the test rod position (Fig. 17). Special equipment for the test consisted of the aluminum rod housing, the stainless-steel rod housing, a cadmium sleeve, and an aluminum bar (Fig. 18). Both rod housings were constructed to the dimension noted on NR1M017, "Rod Assembly - B₄C Shim Safety." The cadmium sleeves were 24 inches long and fitted the inner surface of the housings. The aluminum bar was 24 inches long, 1.365 inches wide, and 0.677 inch thick, and fitted inside the cadmium sleeve.

3.6.2 Procedure

Four parameters were varied during this experiment: two types of rod housings, the cadmium sleeve, and the aluminum bar. Eight possible permutations of the parameters were inserted in location E-4. When criticality was established, the rod configurations were fully retracted from the core and the reactivity worth estimated from the adjusted positions of the other rods. A code for the configurations was established as follows:

HA: aluminum housing

HS: stainless-steel housing

C: cadmium sleeve(X: no sleeve)

A: aluminum bar (X: no bar)

For example, configuration HS-X-A denotes the stainless-steel housing without the cadmium sleeve but with the aluminum bar.

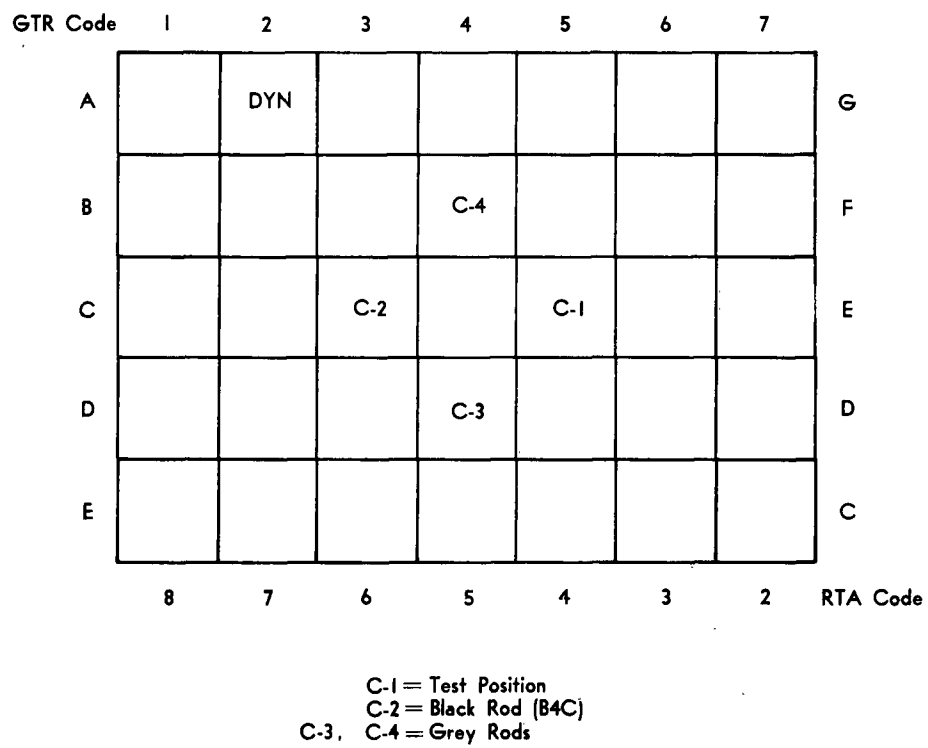


Figure 17. GTR Core with RTA Lattice Locations

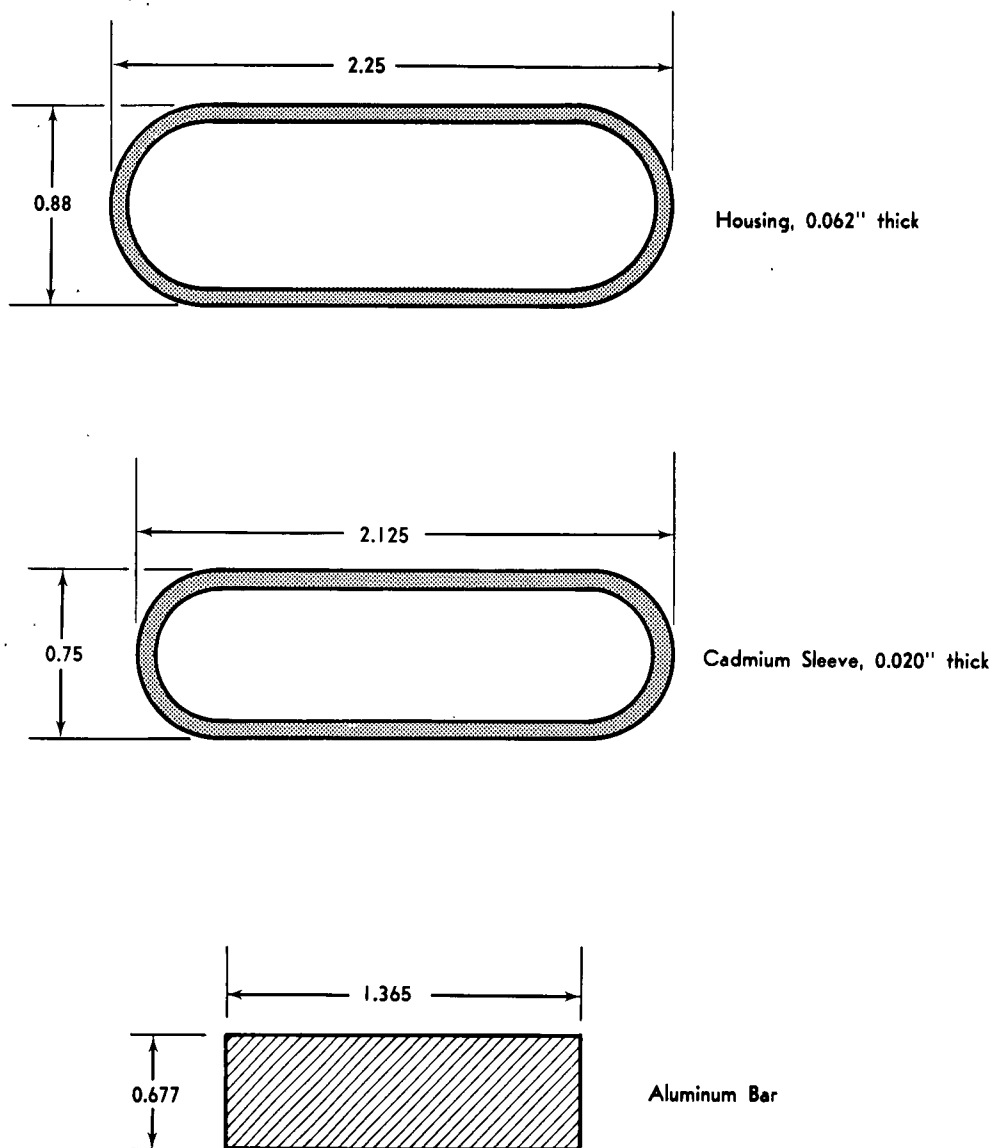


Figure 18. Cross Sections of Test-Rod Components

Following these eight runs, configuration HA-C-X was calibrated by the asymptotic-period method. After this calibration, when the test rod was disassembled, it was discovered that the center of the cadmium sleeve was $13/16$ inch higher than the fuel center. This could affect the overall rod worth. Therefore, the sleeve was repositioned and the rod recalibrated by the period method. The test rod was completely removed from the core and a miniature fission chamber installed in the rod cavity of the control element. The active volume of the fission chamber is a right circular cylinder $3/16$ inch in diameter and 1 inch in length. The fission chamber was traversed through the center of the fuel-element cavity from 0 to 24 inches with the rod-drive mechanism. The chamber was positioned at 1-inch increments and the average count rate determined.

The test-rod configuration HA-C-X was positioned at 12 inches and a fission chamber traverse taken through the core and test rod.

Further experimentation with the test rod was performed on the GTR during January 1962. This information, along with rod calibration and rod drop time, is included for comparison with the RTA experimental values.

3.6.3 Conclusions

The values of the eight possible permutations of the rod parameters are listed in Table V. It is noted that the aluminum rod housing and aluminum bar caused an increase in total core reactivity when they were inserted.

TABLE V
TEST-ROD WORTH

Configuration	Worth
HA-X-X	-0.030%*
HA-X-A	-0.063%*
HA-C-X	2.66%
HA-C-A	2.18%
HS-X-X	0.68%
HS-X-A	.54%
HS-C-X	2.56%
HS-C-A	2.21%

* Minus sign means negative reactivity

The configuration HA-C-X was calibrated by the period method with and without the cadmium liner offset 13/16 inch. The results of both indicated no difference in the total rod worth (2.45% vs 2.42%), as shown in Figures 19 and 20. The fission-chamber measurements (Figs. 21 and 22), indicate the relative thermal-neutron flux in the control-rod position and the relative control-rod absorption in the same position. The point on the control-rod graph indicating the black control-rod 2 position was verified, by repeated traverses, as being a valid point. Figure 22 illustrates the fact that the thermal flux inside the control rod is about 10% of the flux without the cadmium absorber.

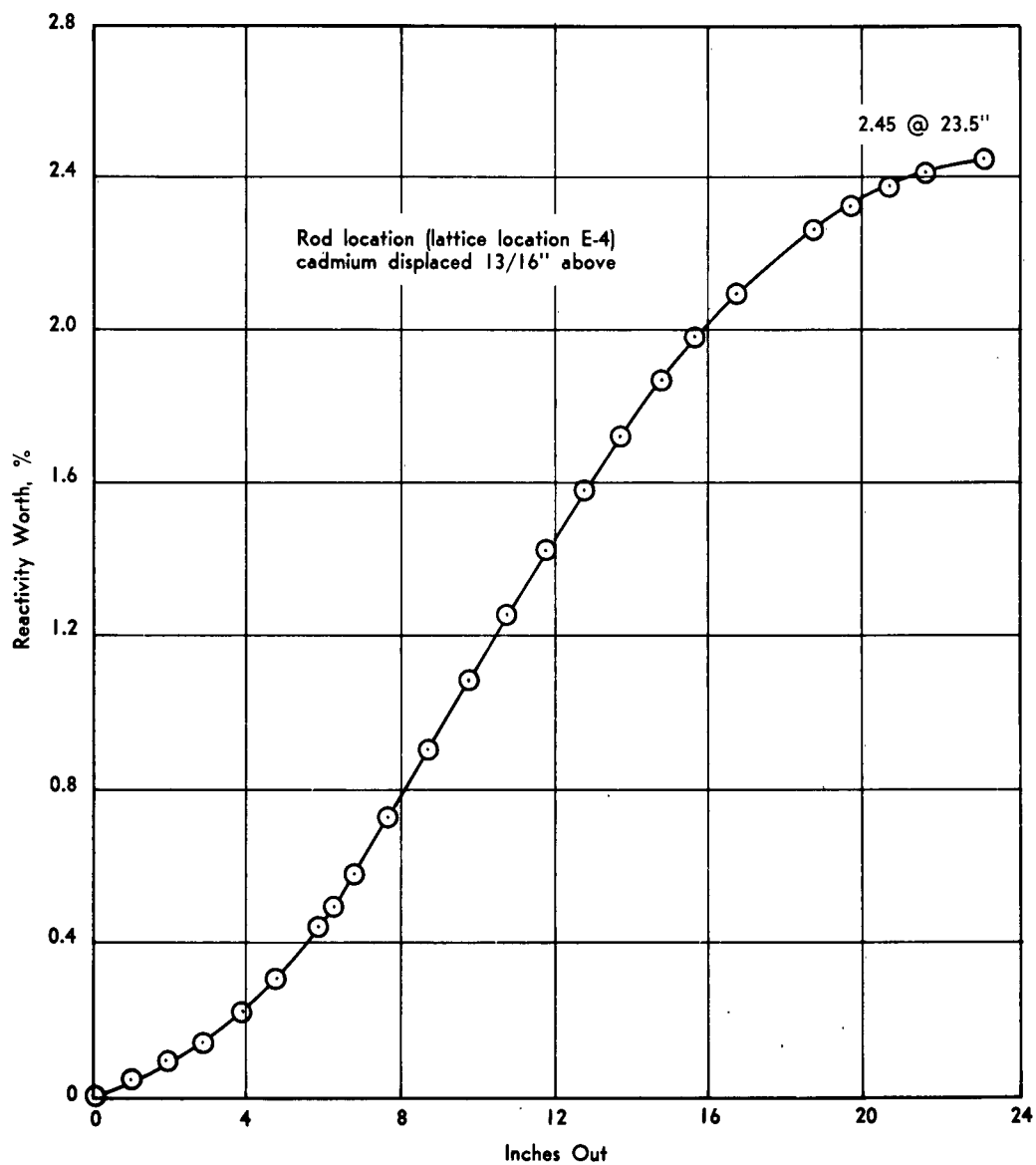


Figure 19. Rod Calibration Curve for GTR Test Rod HA-C-X

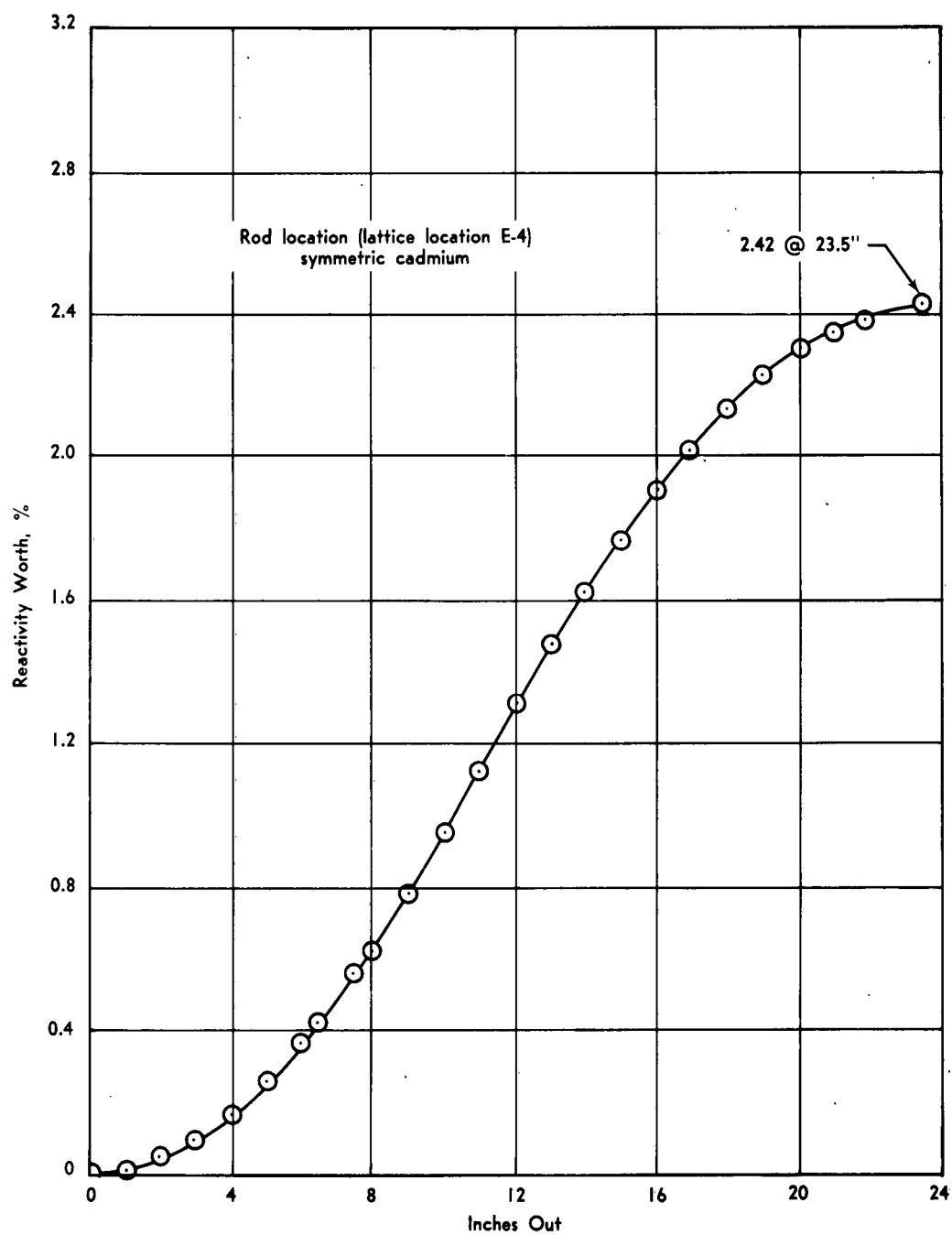


Figure 20. Rod Calibration Curve for GTR Test Rod HA-C' -X

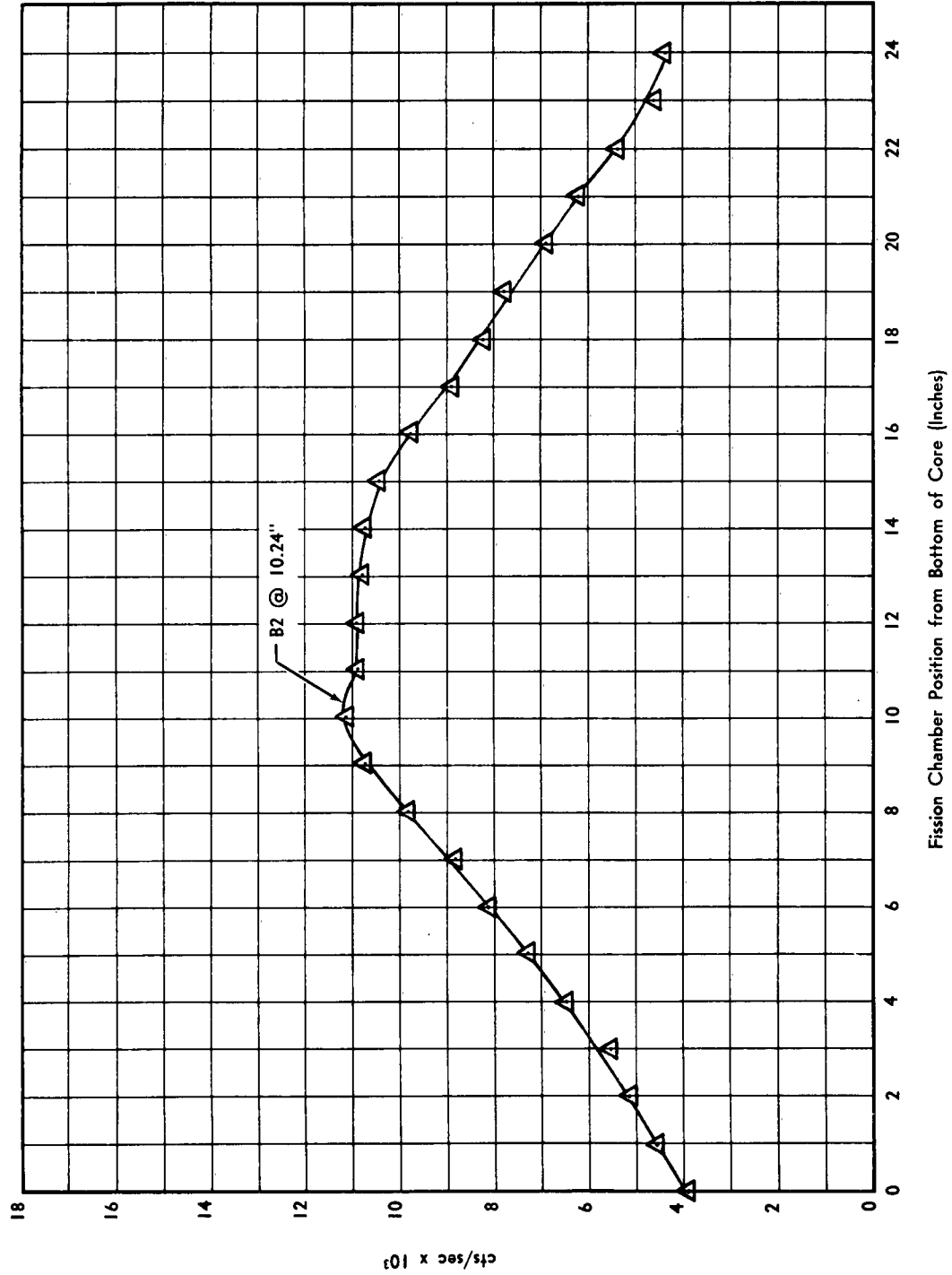
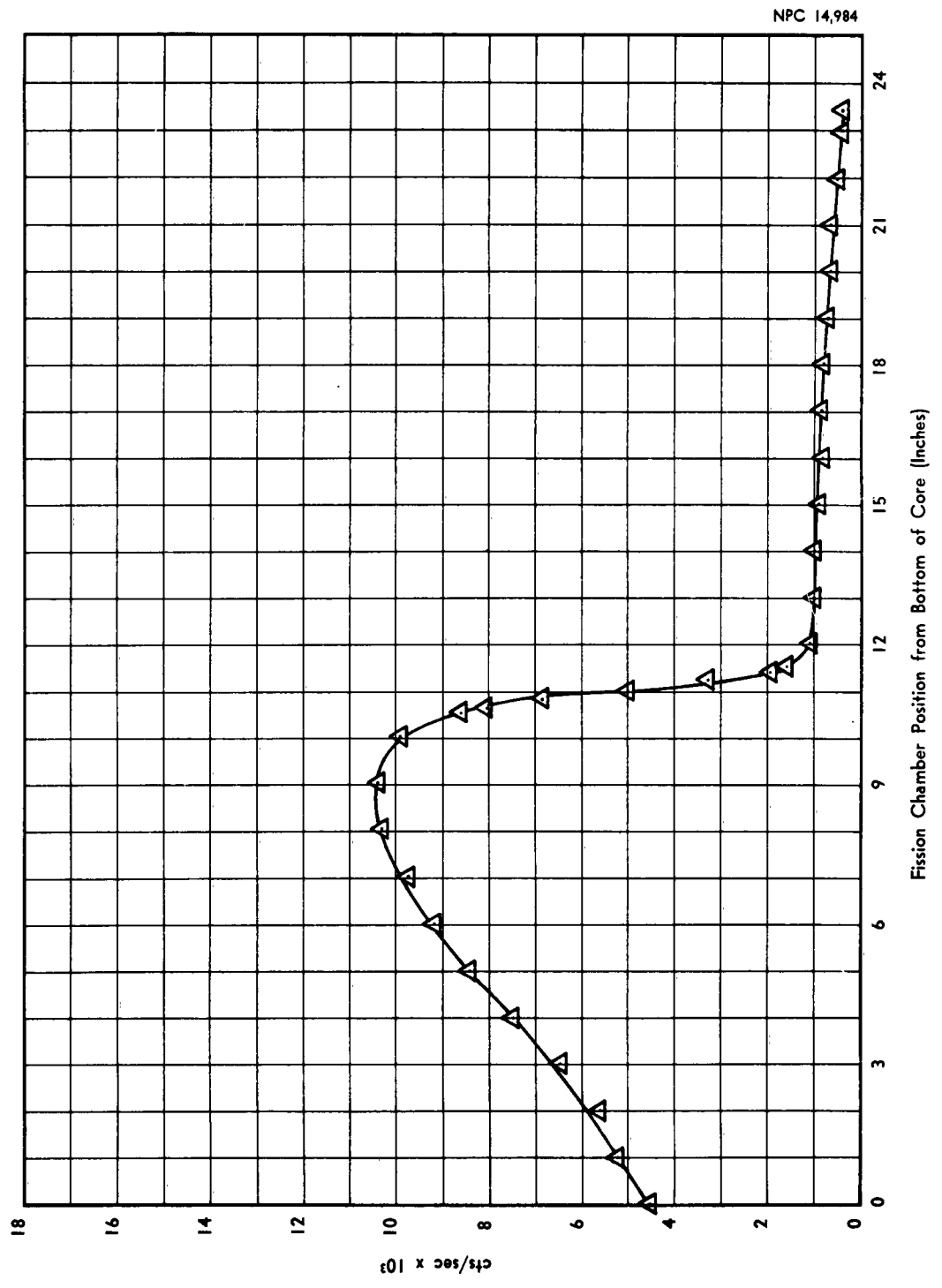


Figure 21. Fission-Chamber Traverse in Control Rod Element



**Figure 22. Fission-Chamber Traverse in Control Rod:
HIA-C-X 12 in. Out**

The rod configuration HA-C-X value as determined in the GTR was 2.37%, which is essentially the value obtained in the RTA (Fig. 23). The rod-drop times of rod configuration HA-C-X were measured from different heights. These values are given in Table VI, along with the drop times for the standard B₄C and dynamic rods for comparison.

TABLE VI
CONTROL ROD DROP TIMES

Rod Type	Drop Distance (in.)	Drop Time (sec.)
Test Rod	8	0.35
	16	0.44
	23.5	0.52
B ₄ C Black Rod	23.5	0.50
Dynamic Rod	23.5	0.52

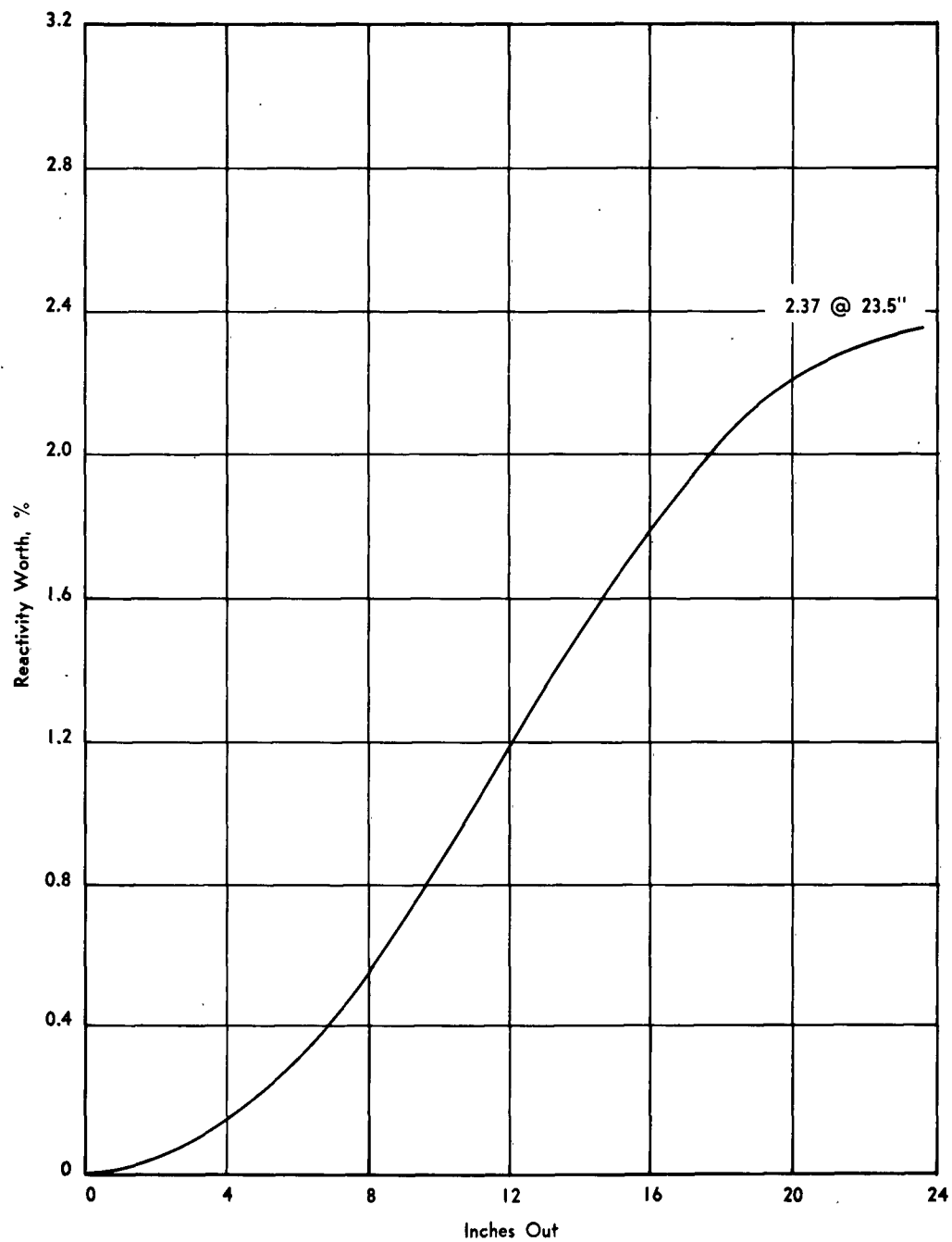


Figure 23. Rod Calibration of HA-C-X in GTR

3.7 Moderated-Fast-Section Reactivity Measurement

3.7.1 Experimental Equipment

The normal 5 x 7 GTR core loading was set up in the RTA grid in an offset position to achieve a large available volume in the reflector. The reflector thickness available for this experiment was approximately 12 inches. The configuration to be simulated was the GTR and the pool separator, with a given quantity of U²³⁵ on the dry side of the pool adjacent to the core. This configuration involved only those measurements simulating flooding of the entire assembly.

The pool separator was simulated by a 26- by 29-inch by 1-inch-thick sheet of aluminum. Provisions were made to hold the U²³⁵ assemblies in contact with one face of the plate. The U²³⁵ was assembled in the form of standard GTR elements (140 gm). A total of seven elements were used, three of which were assembled from fuel plates and side plates on hand and the remainder of which were manufactured GTR elements.

3.7.2 Procedure

The core reactivity was measured, and the number of cadmium poison strips necessary to lower the available core reactivity to approximately 1.5% $\Delta k/k$ was determined. After some manipulation of the poison strips, a uniform distribution achieved a core reactivity of 1.60% $\Delta k/k$. This core configuration was used throughout the experiment (Fig. 24).

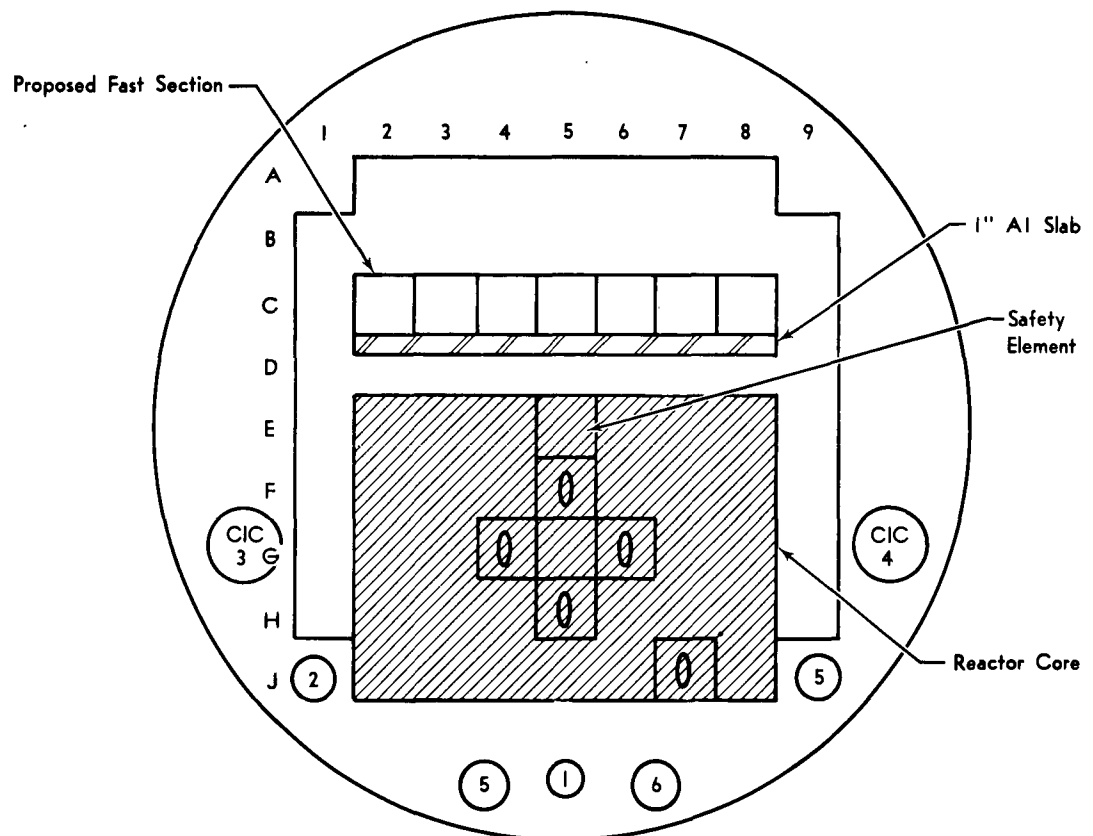


Figure 24. Core Geometry for Flooded Fast-Section Measurements

The pool separator mockup was positioned first in such a way that there was a distance of two inches between the core face and the pool separator. The core reactivity of this configuration was measured. The aluminum plate was removed and one fuel element positioned in the center of the plate against the outer surface. The plate was then repositioned at two inches and the core reactivity measured. Succeeding steps were performed by adding two fuel element assemblies each time and measuring the reactivity of the assembly. The reactivity measurements were calculated from control rod positions. The final assembly contained seven elements.

The entire assembly - i.e., aluminum plate and seven elements - was repositioned for separation distances of three and five inches, where reactivity measurements were made. The plate-and-fuel-element assembly was removed from the RTA and a sheet of 0.020-inch-thick cadmium attached to the plate side adjacent to the core and covering the area of the plate. This cadmium-covered assembly was repositioned at two inches and the reactivity measured.

3.7.3 Conclusion

The reactivity measurements for the fast-fission section in a moderated condition are shown in Figure 25. The reactivity value at the two-inch position was determined to be $1.09\% \Delta k/k$. The cadmium poison sheet was found to be equivalent to approximately three inches of water as a decoupling region. The reactivity values measured throughout the experiment are in Table VII.

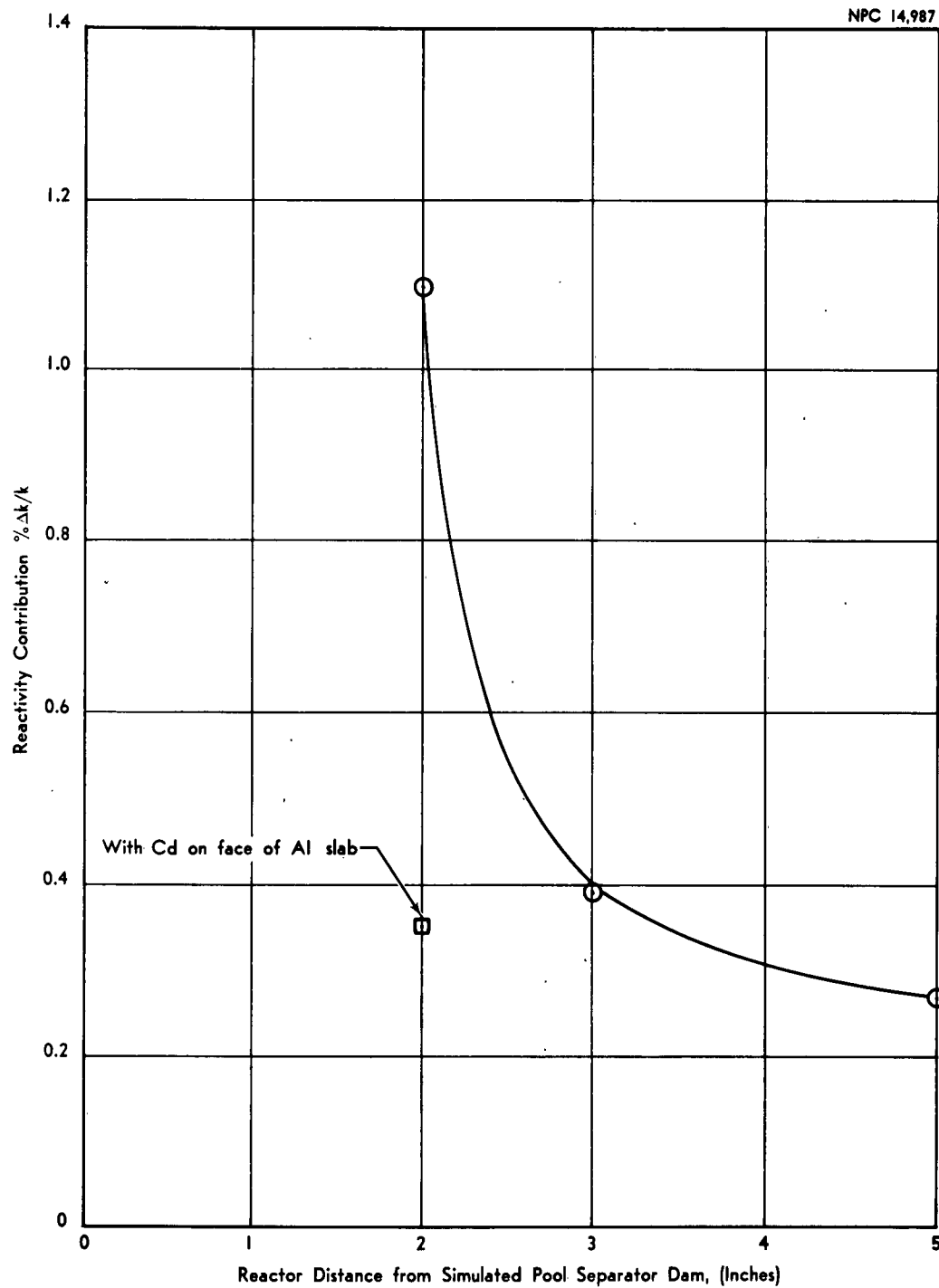


Figure 25. Reactivity vs Distance between GTR and Flooded Fast Section

TABLE VII
REACTIVITY CONTRIBUTION OF FLOODED FAST SECTION

Description	Reactivity($\Delta k/k$)
1-in. Al plate @ 2 in.	+0.06%
Al plate + 1 fuel element @ 2 in.	+0.33
Al plate + 2 fuel elements @ 2 in.	+0.48
Al plate + 3 fuel elements @ 2 in.	+0.68
Al plate + 5 fuel elements @ 2 in.	+0.91
Al plate + 7 fuel elements @ 2 in.	+1.09
Al plate + 7 fuel elements @ 3 in.	+0.39
Al plate + 7 fuel elements @ 5 in.	+0.27
Al plate + cadmium + fuel elements @ 2 in.	+0.36

IV. ASTR EXPERIMENTS

4.1 ASTR-Core Critical Experiment and Loading Adjustment

4.1.1 Experimental Equipment

Normal RTA startup instrumentation was utilized with the detectors positioned as shown in Figure 26, Loading 1. The rod drives were relocated on the control platform to conform with the geometry of the 3-Mw ASTR. Three new ASTR rod assemblies were installed in the grid plate and cycle-tested for proper operation before any fuel was added. An ASTR three-quarter element was installed on the lower half of the center safety rod. The entire assembly was then installed in the tank.

4.1.2 Procedure

The BF_3 detectors (Channels 1, 1A, and 2) were source-checked, a background (C_b) and source count (C_s) were taken, and the tank was drained in preparation for the first loading. Loading 1 (Fig. 26) consisted of 8 full elements, 1 three-quarter element, and 2 dummy elements. Both rods-in and rods-out count rate (C_m) were obtained and the ratio C_s/C_m (reciprocal multiplication) for each plotted in Figures 27 and 28, respectively. The loading steps proposed in the planning document were followed and are shown (Fig. 26) up to and including the critical loading, No. 11. Criticality was predicted by previous experiments and by calculations to occur at Loading 9. An investigation at this point did not show the reason criticality required 300 gm more fuel than predicted. The remaining two elements were added

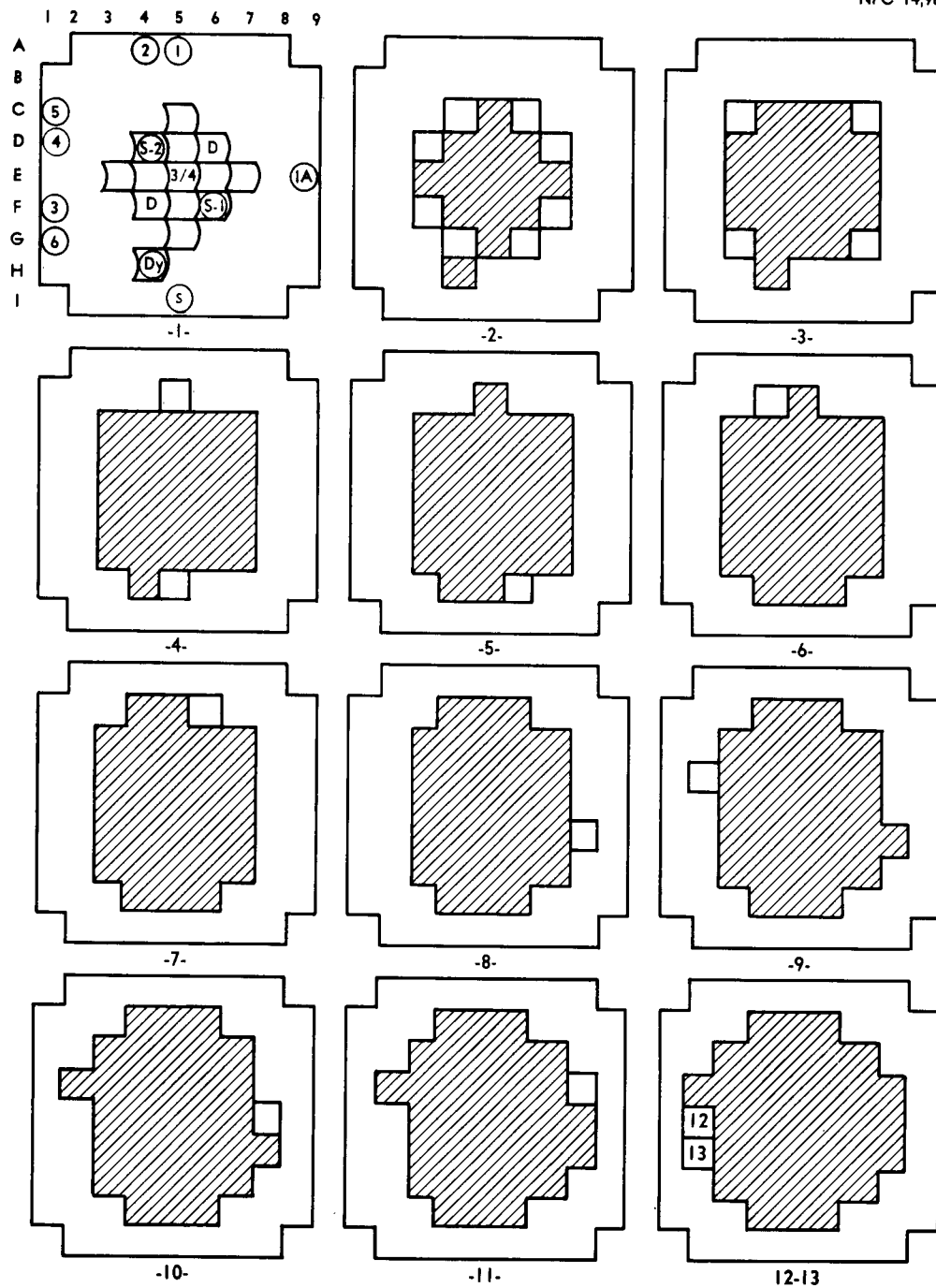


Figure 26. ASTR Critical-Experiment Loading Sequence

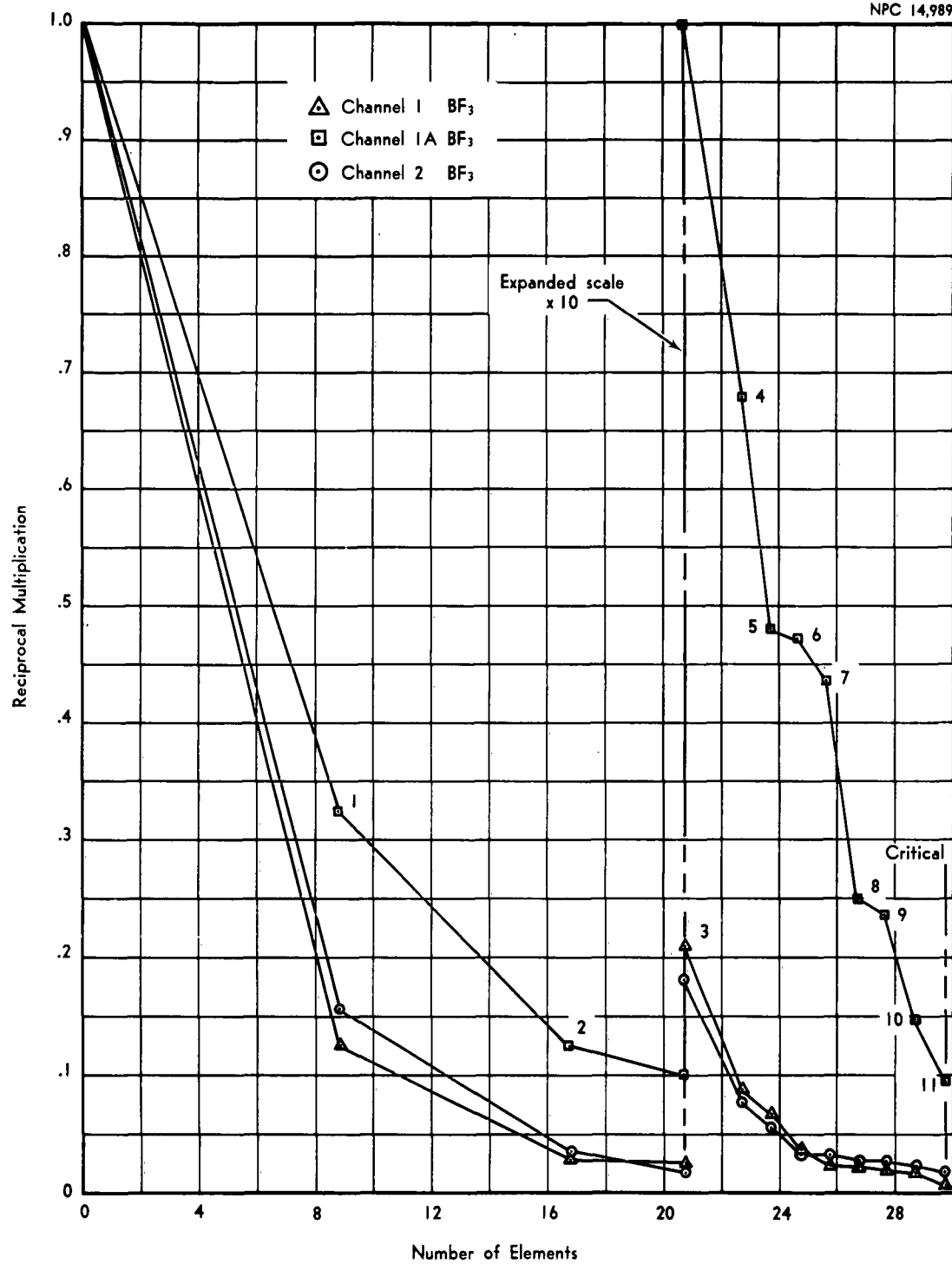


Figure 27. ASTR Rods-in Reciprocal Multiplication Curves

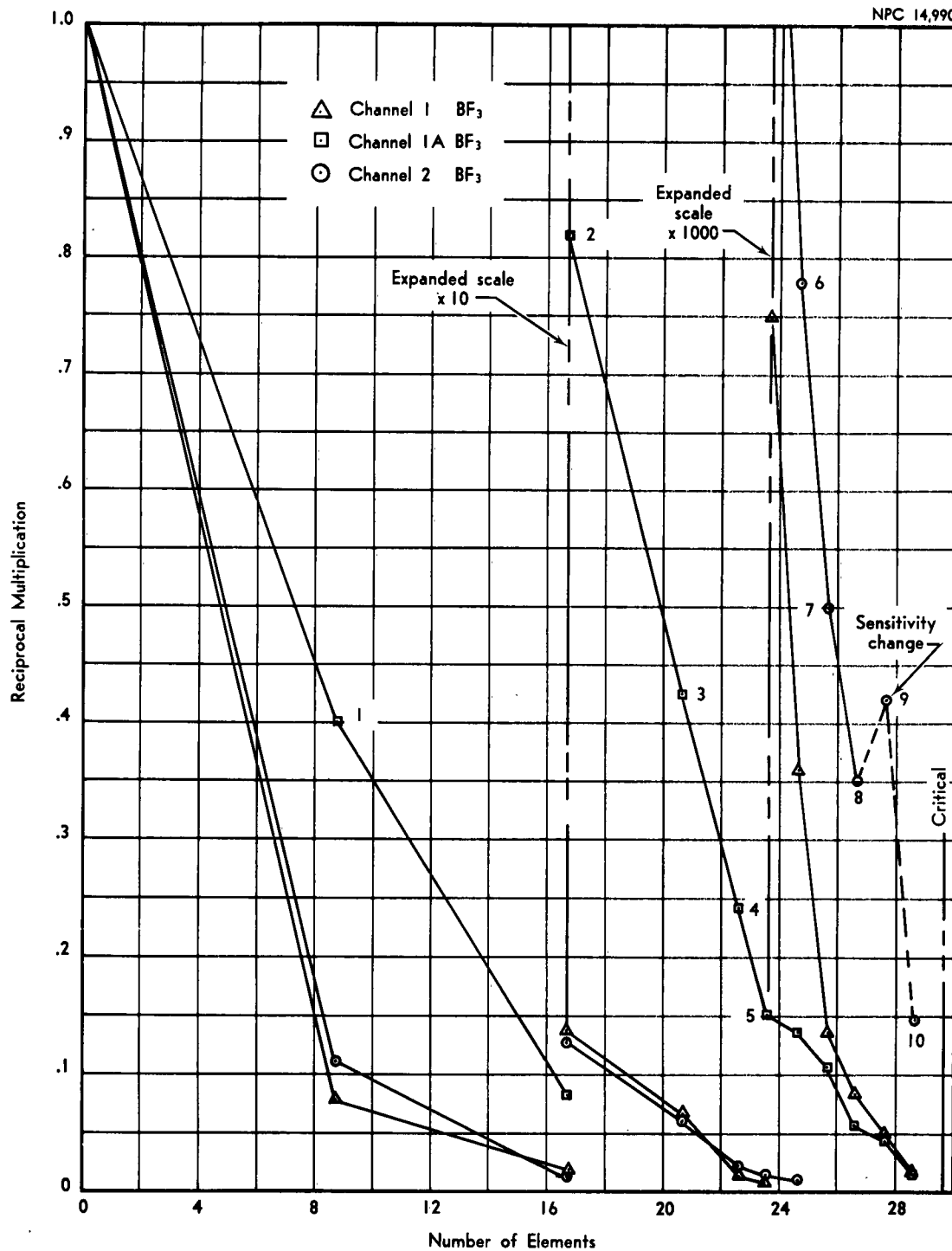


Figure 28. ASTR Rods-out Reciprocal Multiplication Curves

singly to the critical configuration to complete the 3-Mw core loading (Fig. 26, Loadings 12 and 13). A preliminary rod calibration showed reasonable agreement with previous calibrations of identical rods.

However, an excess reactivity of 1.82% was determined from critical-rod positions, whereas the previous ASTR core in the identical configuration possessed on the order of 2.5% excess reactivity. An investigation was begun to account for the observed discrepancies. Several tests were performed in order to determine the reactivity effect of (1) detector location in reference to fuel, (2) poison due to control-rod housings, (3) variation between dummy elements with different construction, and (4) poison due to structural aluminum in the elements. These tests are described below.

The detectors were moved further from the reactor core in the reflector region (Fig. 26, Loadings 12 and 13). This produced no significant change in core reactivity.

One spare control rod was substituted in the core for each control rod, in turn, and the removed rod was disassembled. The reactivity worths of the three rod-housing structures were checked in the reactor dummy positions. The structure worths were not significantly different from the values obtained with previous rod-housing structures.

The RTA dummy elements used in the ASTR core mockup were not made of the same type of material as the 3-Mw ASTR dummy elements. The reactivity values of the RTA dummies were found to lower the core reactivity by 0.2% $\Delta k/k$.

The fuel elements were checked for discrepancies in fuel loading and poison materials by cycling four fuel elements from the periphery to the center of the core and measuring the core reactivity for each cycle. The reactivity values for cycles were within 0.1% $\Delta k/k$.

Comparison of the method of manufacture of these elements and previous ASTR elements revealed two major differences that would tend to cancel each other:

1. Although all elements have the specified element loading (150 gm U^{235} , $\pm 1\%$), they all have a positive loading tolerance (+1.35 to +1.50 gm).
2. The elements are assembled by mechanical means (pinned) with 6061-T6 aluminum pins and side plates rather than by brazing with 1100-2S aluminum side plates and brazing flux.

The remaining 0.6% difference in reactivity can be attributed to this change in fabrication methods.

The ASTR core was adjusted to 2.43% $\Delta k/k$ by removing the three-quarter element from the center of the core and by replacing it with a full fuel element - a total mass of 4830 grams of U^{235} .

4.1.3 Conclusion

The ASTR core configuration in the RTA was made critical at 4:00 p.m., 17 May 1961. The loading consisted of 29 full elements and one partial (three-quarter) fuel element — a total mass of 4490 grams of U^{235} . The loading sequence to criticality was accomplished in 11 steps. The observed critical mass did not agree with previous ASTR critical mass experiments or with calculated values.

The loading adjustment to the full 3-Mw core loading of 4790 grams of U²³⁵ provided almost 1% less reactivity than anticipated. Subsequent investigation disclosed that a loss of 0.62% reactivity was due to the substitution of 6061-T6 aluminum for 1100-2S in the side plates. Approximately 0.2% loss in reactivity was due to the manner of construction of RTA dummies. Accordingly, a full element was substituted for the three-quarter element in the center location of the core.

4.2 ASTR Rod Calibration

4.2.1 Experimental Equipment

The experiment used the modified ASTR core loading (Sec. 4.1), which gave a reactivity of 2.5% $\Delta k/k$. This loading consisted of 32 full elements and two dummies. The three control rods were manufactured spares for the ASTR and had not been previously calibrated. The normal RTA instrumentation was used during this experiment.

4.2.2 Procedure

The three control rods were evaluated by correlating incremental rod movement with the resulting stable period by use of the In-Hour relationship. The RTA was brought critical and the source removed. A long period was established as a base reference. The rod being calibrated was then withdrawn a given increment and the resulting stable period measured. Previous experimental data have revealed that rod shadowing between the two safety rods does not occur in sufficient magnitude to be measured. As a result of the lack of shadowing effects, no poison strips were required during the ASTR rod calibrations.

The safety-element value was estimated by withdrawing all control rods while the safety element remained inserted and by measuring the shutdown multiplication. The shutdown multiplication, along with knowledge of the core excess reactivity, made it possible to estimate the safety-element worth.

4.2.3 Conclusion

The worth of the three ASTR rods is shown in Figure 29. The fact that S-2 was worth more than S-1 is probably a result of the core geometry and was evident again when the original ASTR rods were calibrated in the new core. The safety-element value was approximately $8\% \Delta k/k$.

4.3 Four-Rod ASTR and Void Configurations

4.3.1 Experimental Equipment

The equipment used during this experiment was the ASTR core III, normal RTA instrumentation, two additional ASTR control rods, and the ASTR reflector void.

The additional control rods were disassembled and inspected. When the control rods were reassembled, one contained no poison sleeve, and the other was a standard control rod.

The ASTR void can is constructed from aluminum, with the top and bottom machined from 1/8-inch aluminum stock and the sides fabricated from 1/16-inch-thick aluminum sheet (Fig. 30). Extending from the top of the void assembly was a 1-inch pipe which was used for air pressure and handling. The void dimensions were dictated by the space available between the ASTR core and the pressure vessel. The void is 9 inches wide, 16 inches in

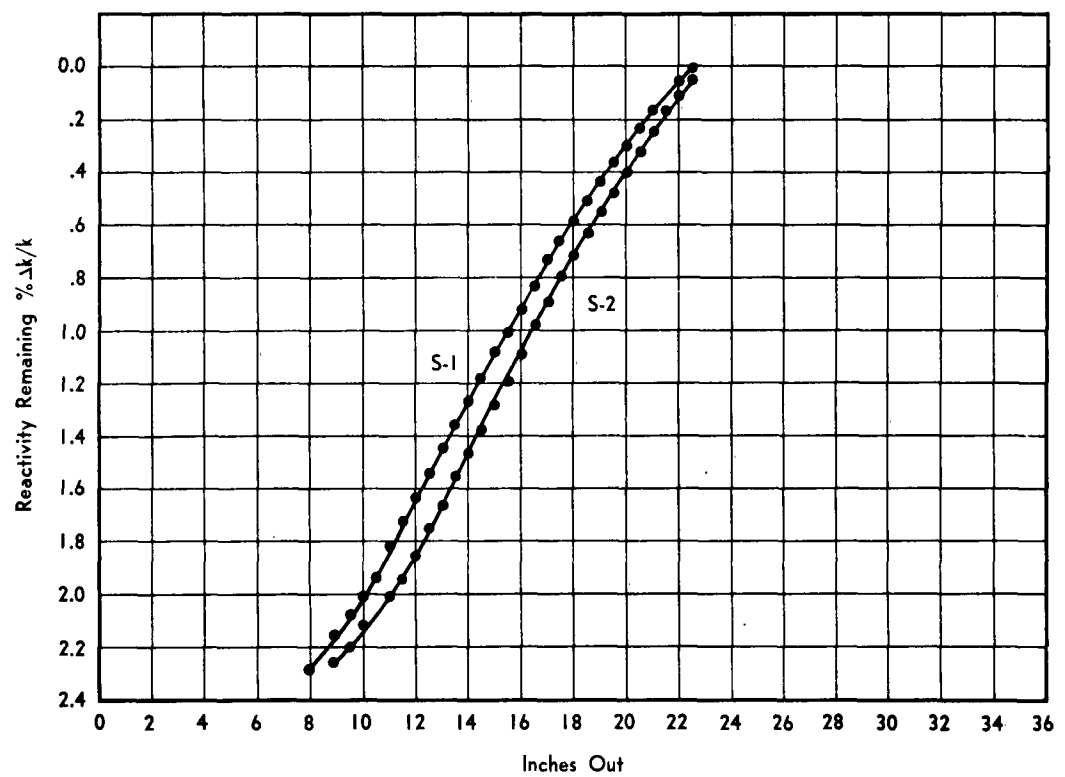
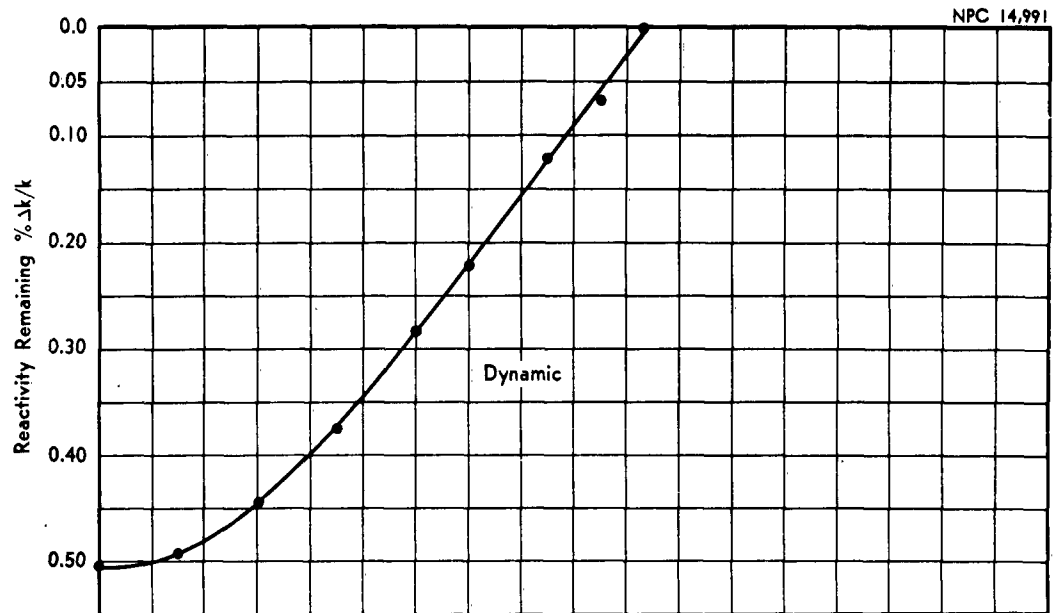


Figure 29. Safety-and Dynamic-Rod Calibration

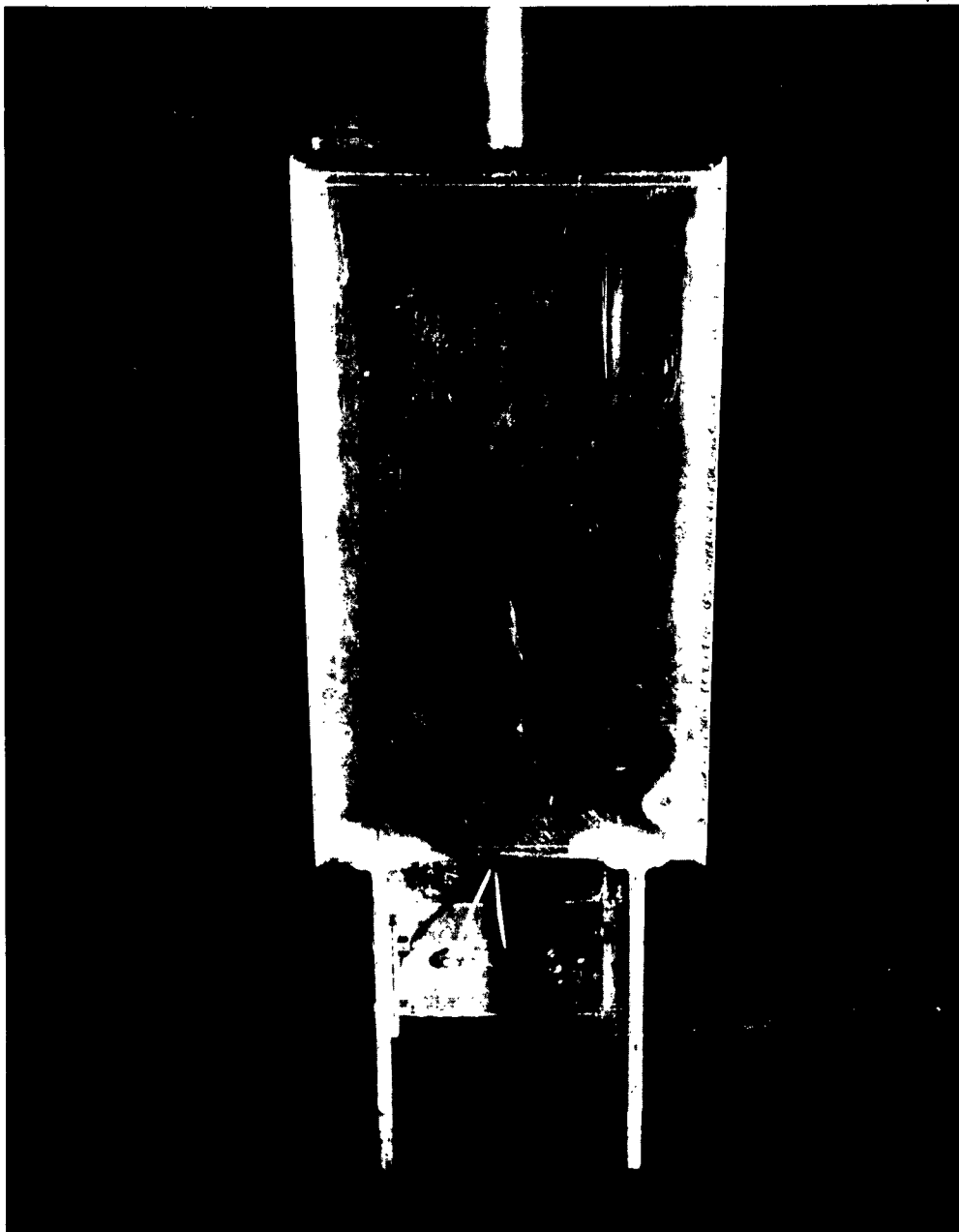


Figure 30. ASTR Reflector Void

height, and 4.63 inches deep at the largest cross section. The curved side has a 16-inch radius. The void was equipped with two legs which fit the gridplate holes and provide accurate positioning. Lead ballast was attached to these legs to ensure that the void could not float.

4.3.2 Procedure

The ASTR core was assembled in the RTA tank, and a criticality measurement (Fig. 31, Loading 1) - called the base measurement - was made. One dummy element was removed and the criticality value of the core measured. The next core reactivity measurement was made with a rod structure in the position of the dummy element which had been removed earlier. The preceding measurements were made in preparation for the 4-rod ASTR configuration.

The 4-rod ASTR configuration (Fig. 31, Loading 4) was constructed by removing both dummy elements and placing a control rod (with poison) in one dummy location and a full element in the other. The control rod which was added had no drive and, hence, was left in the full-in position. Criticality was achieved by withdrawing the remaining three control rods. The reactivity values were computed from the three calibrated rods and a value assumed for the fourth rod. The assumed value for the fourth rod ($3.1\% \Delta k/k$) was arrived at through extrapolation of the calibrated rod curves to a rod-in value. Rod calibrations by the period method were performed for the three control rods during the 4-rod ASTR configuration operation. The value of the dynamic changed, but little change was noticed in the safety rods.

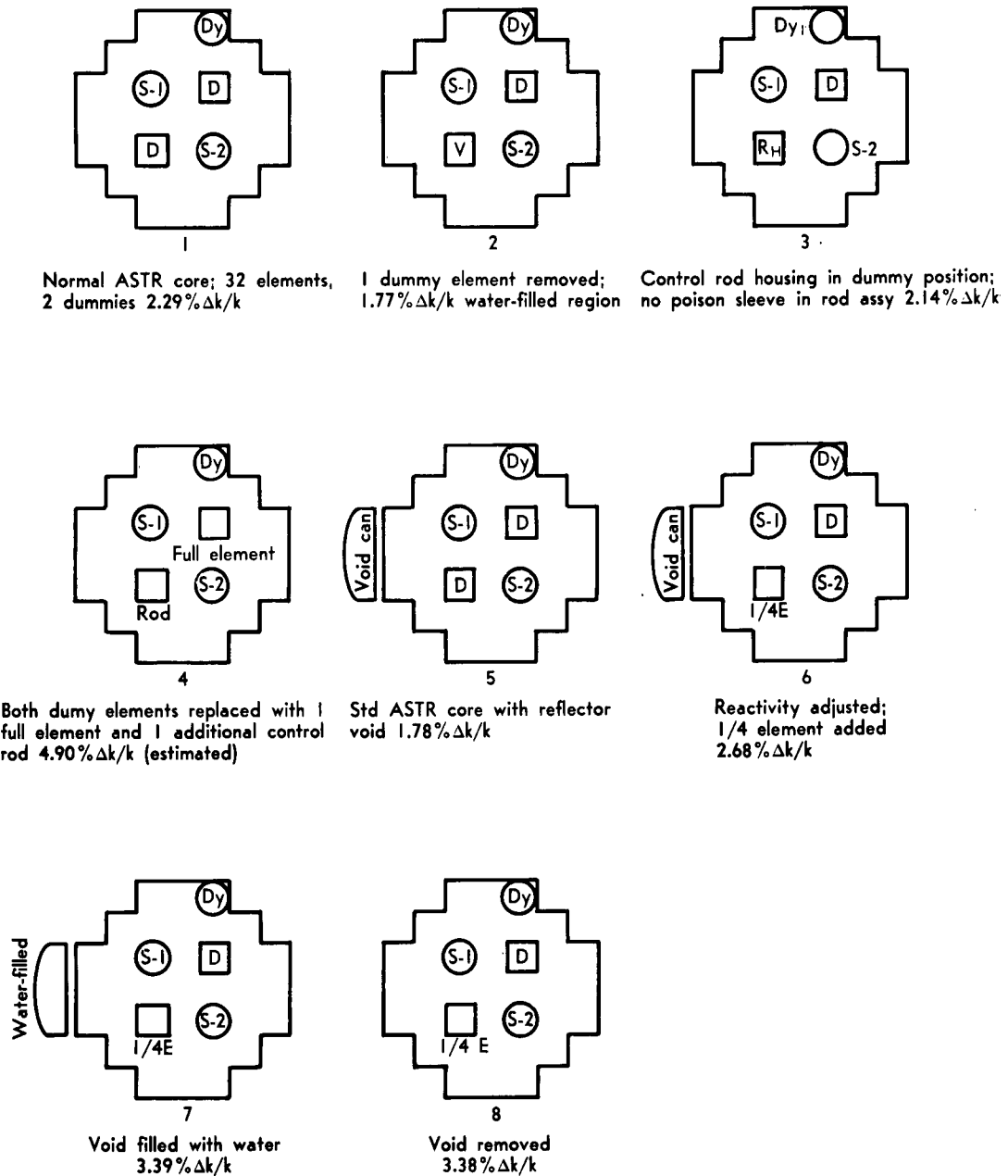


FIGURE 31. ASTR Control-Rod and Void Configurations

The 4-rod configuration was modified back to the original 3-rod configuration with a reflector void along a 3-element face of the core (Fig. 31, Loading 5). This void face was 1/4 inch from the core face. During the air void portions of the experiment, air pressure in the void was maintained at 7 psig. To regain the reactivity lost as a result of the void, a quarter element was placed in the dummy position adjacent to the void face of the core (Fig. 31, Loading 6), thus increasing the reactivity to the approximate operating value of the present 3-Mw ASTR.

The leakage flux into and from the void was measured with sulphur, gold, and cadmium-covered gold. The foils were positioned as illustrated in Figure 32, with the sulphur in the center having a bare and cadmium-covered gold foil on each side. The outside face (Face B) was covered entirely with a sheet of 20-mil cadmium to simulate an air environment outside of the void relative to thermal neutrons. To establish the perturbation effect of the aluminum in the void can, two reactivity measurements were made: one with the void filled with water, the other with the void removed from the core (Fig. 31, Loadings 7 and 8).

4.3.3 Conclusions

The data reveal that a 4-rod ASTR configuration would give an operating reactivity of approximately 5%, with a control rod worth of 9.5%.

The data from the void measurement reveal an increase in the leakage flux from the core by voiding a section of the reflector. The data for these measurements are given in Figure 32.

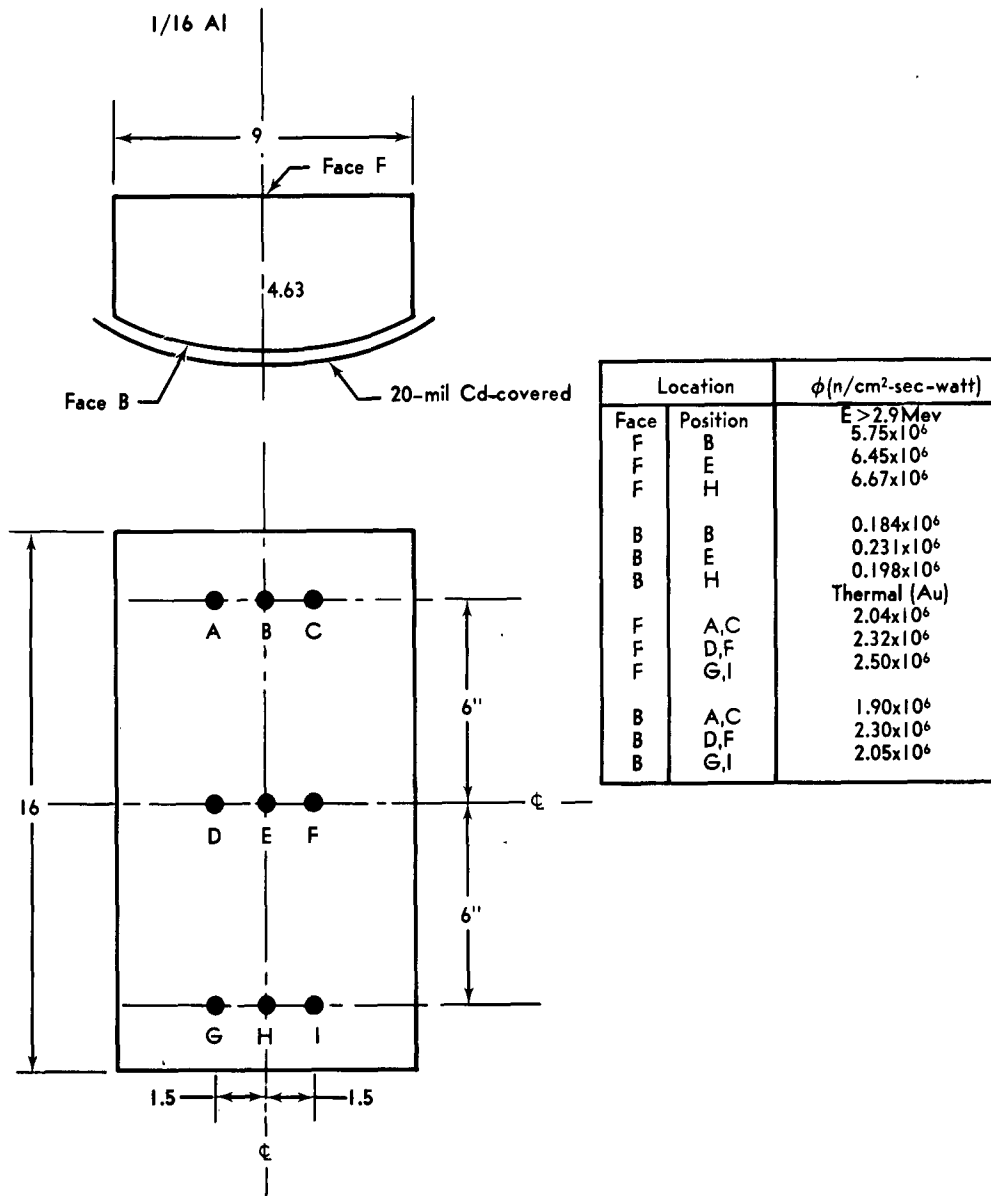


FIGURE 32. Flux Measurements in ASTR Void

4.4 ASTR Core Thermal-Neutron Flux Measurements

4.4.1 Experimental Equipment

The equipment used to measure thermal-neutron flux was gold foil, cadmium covers for the foils, copper wires, and the necessary equipment for the proper positioning of the foils and wires.

The gold foils were circular, two mils thick, and had a weight of approximately 0.1 gm. The cadmium covers were 20 mils thick and of sufficient diameter to cover the gold foils. For measurements along the axial centerline of the fuel elements, the gold foils were positioned by taping to a plexiglas stringer. For measurements on the exterior of the fuel elements, the foils were affixed directly to the side of the element with tape. The copper wires were 0.051 inch in diameter and 33 inches long. They were positioned along the axial centerline by placing the wires between plates and by the use of polyethylene retainers at each end of the element.

4.4.2 Procedure

The experimental procedure was divided into two parts. The first was the irradiation of two gold foils, one bare and one cadmium-covered, and one copper wire in each fuel element location; the second, the irradiation of bare gold foils at 25 selected locations in each of 12 selected lattice locations (Fig. 33). Two cadmium-covered foils were also irradiated at the same 12-lattice locations.

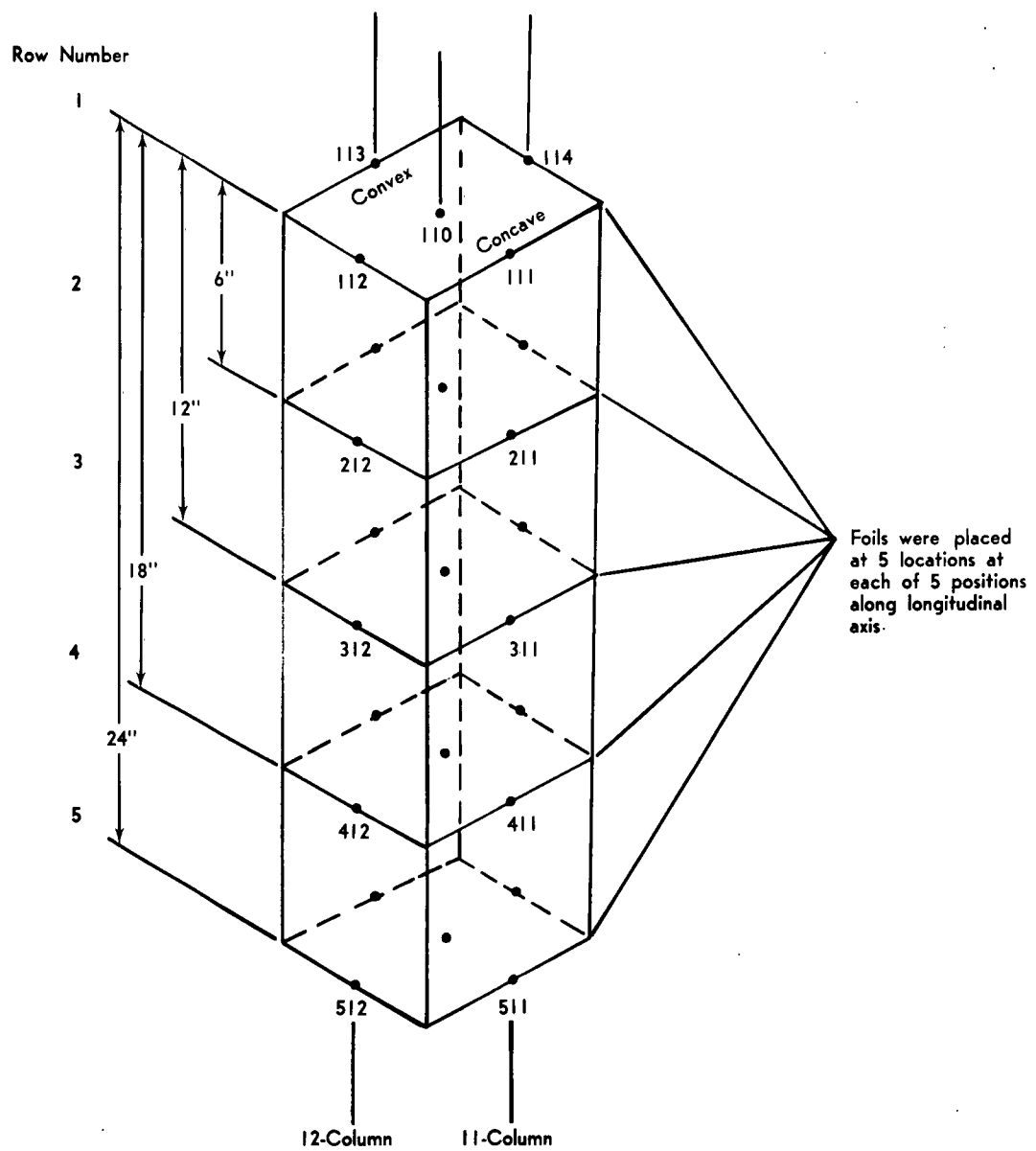


Figure 33. Foil-Position Code on Fuel Element

The first part, hereafter called the "standard method," commenced with the irradiation of the bare gold foils located at the center of the elements. This was accomplished in five separate reactor operations in order to minimize flux perturbations. The reactor was operated at 10 nominal watts for 10 minutes and then shut down. The cadmium-covered foils were irradiated in seven separate runs, the greater number of runs being required to reduce flux perturbation. Copper wires were irradiated along the axial centerline of the element in five separate runs. Both foils and wires were delivered to the counting room for counting.

The second part of the experiment, hereafter termed the "refined method," required 36 separate reactor operations. For the purposes of designation of foil location, a number code was adopted as shown in Figure 33. It should be noted that the top of the element in the RTA is on the same end of the core as the withdrawing rods. Thus, the top of the RTA corresponds to the aft end of the ASTR, in the manner that flux is perturbed by the rods. As shown in Figure 33, the fuel element was divided into five columns, numbered zero (for axial center), 1 (for concave side), 2 and 4 (for flat sides), and 3 (for convex side). The rows are numbered 1 through 5 to designate zero inches, 6 inches, 12 inches, 18 inches, and 24 inches, respectively, from the aft end of the fuel.

Each of the first 30 runs of the refined method consisted of irradiation of one column in each of two locations. The 12 selected locations are shown in Figure 34. The selection of these locations was on the basis of core symmetry; for example, lattice locations

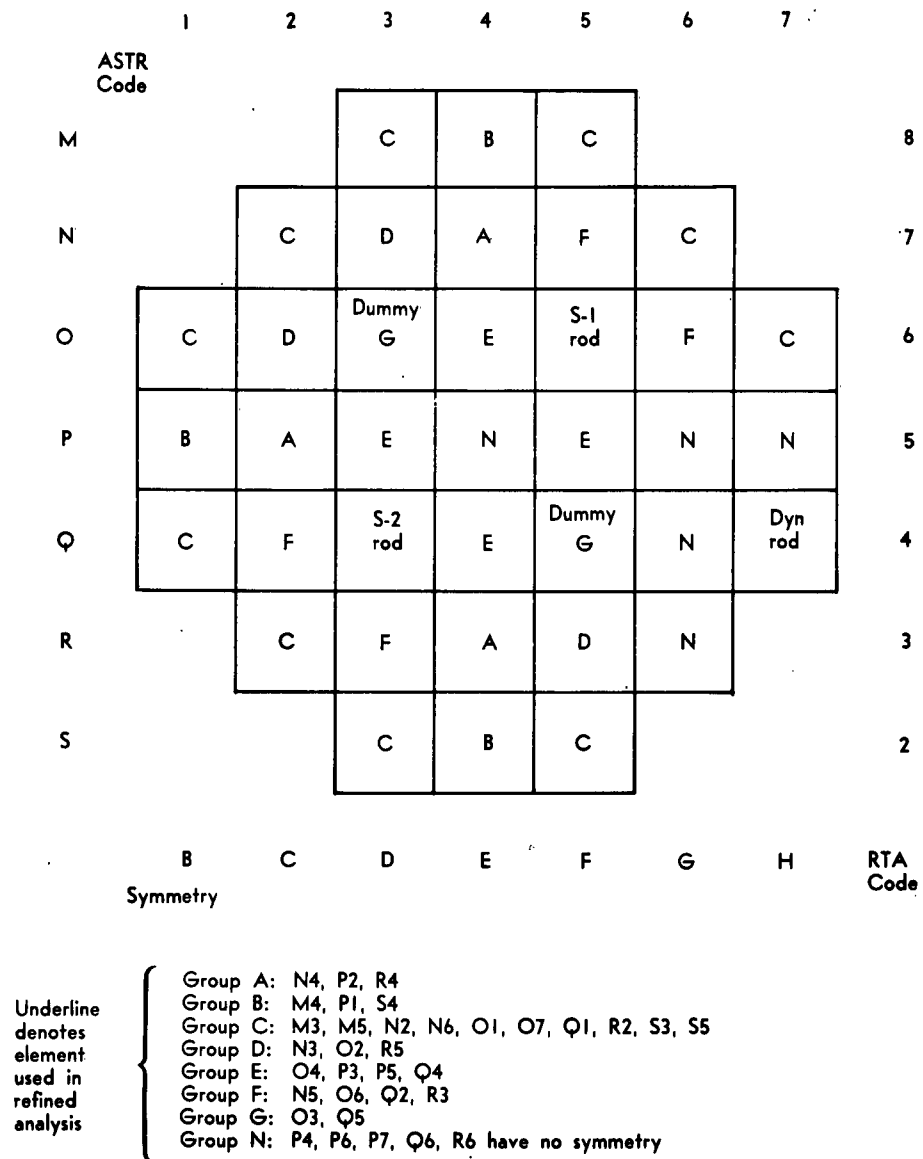


FIGURE 34. ASTR Lattice Diagram with Symmetry Assumptions

N-3 and O-2 are both next to a dummy element, with one element removed from the core face. Five elements were assumed to have no symmetry. The last six runs consisted of the irradiation of cadmium-covered foils at the 110 and 510 locations on each of the 12 selected elements.

The activated foils were counted by the counting room; the counting results were reduced to saturated activities by a computer program. Thermal flux was not computed, inasmuch as it was not practical to irradiate both bare and cadmium-covered foils at the same place at the same time.

The counting rate on the copper wires was observed by passing the copper wire through a scintillation crystal at a uniform rate and recording the detected disintegrations on a strip-chart recorder. Only relative count rates were required, since the only item of interest from the copper wires is the relative intensity of axial neutron flux.

4.4.3 Conclusion

The results of the standard-method measurements are listed on Tables VIII and IX. In Table VIII the bare and cadmium-covered saturated activities are itemized for each lattice location. The thermal saturated activity, which is the difference between the bare and cadmium-covered, is also listed in Table VIII, together with other calculations which are explained in Section 4.4.3.1.

The relative copper-wire activities are itemized in Table IX. There are no units on these numbers and the numbers for one location may not be compared with those for another location, since different delay times and scale factors were involved.

TABLE VIII

POWER GENERATION AS DETERMINED BY STANDARD METHOD

ASTR Lattice Location	Bare Saturated Activity (x 10 ¹⁰) (dpm/gm-w)	Cd-Covered Saturated Activity (x 10 ¹⁰) (dpm/gm-w)	Thermal Saturated Activity (x 10 ¹⁰) (dpm/gm-w)	$\phi_{avg}/\phi_{\bar{g}}$	Average Thermal Saturated Activity (x 10 ¹⁰) (dpm/gm-w)	Element Contribution (%)
M3	.323	.119	.204	.792	.162	2.59
M4	.316	.120	.196	.794	.156	2.49
M5	.289	.107	.182	.793	.144	2.30
N2	.389	.141	.248	.780	.193	3.08
N3	.449	.147	.302	.772	.233	3.71
N4	.461	.162	.299	.788	.236	3.75
N5	.369	.134	.235	.795	.187	3.02
N6	.320	.108	.212	.796	.169	2.70
O1	.369	.127	.242	.799	.193	3.08
O2	.497	.180	.317	.796	.252	4.01
O4	.582	.185	.397	.787	.312	4.95
O6	.322	.122	.200	.788	.158	2.52
O7	.222	.099	.123	.801	.099	1.58
P1	.407	.095	.312	.784	.245	3.90
P2	.409	.157	.252	.784	.198	3.15
P3	.558	.178	.380	.795	.302	4.80
P4	.534	.197	.337	.780	.263	4.18
P5	.473	.175	.298	.783	.233	3.71
P6	.420	.138	.282	.786	.222	3.53
P7	.194	.094	.100	.814	.081	1.31
Q1	.316	.087	.229	.781	.179	2.85
Q2	.434	.133	.365	.783	.222	3.57
Q4	.511	.191	.320	.756	.242	3.85
Q6	.295	.108	.187	.791	.148	2.37
R2	.339	.082	.257	.786	.202	3.22
R3	.405	.131	.274	.787	.216	3.44
R4	.417	.153	.264	.795	.210	3.34
R5	.363	.143	.220	.797	.175	2.79
R6	.285	.105	.180	.814	.147	2.35
S3	.303	.082	.221	.797	.176	2.81
S4	.304	.102	.202	.797	.161	2.57
S5	.295	.097	.198	.786	.156	2.49

TABLE IX
RELATIVE COPPER-WIRE ACTIVITIES

Lattice Location	Distance From Forward End (in.)																								
	Forward End												Center				Art End								
	0	1	2	3	4	5	6	7	8	9	10	11	12	13	14	15	16	17	18	19	20	21	22	23	24
M3	380	341	328	363	400	438	474	511	518	528	551	556	550	550	536	515	484	449	415	375	336	318	283	286	315
M4	409	372	350	386	430	491	524	558	573	585	590	604	588	585	575	548	511	470	444	398	358	312	279	298	344
M5	315	288	280	290	322	345	377	406	418	455	450	448	432	422	415	398	375	354	325	295	256	235	220	232	248
N2	501	455	458	480	538	597	637	668	694	715	725	743	737	714	689	673	635	594	538	503	448	386	346	374	409
N3	498	440	420	446	493	550	591	632	641	664	671	684	690	667	645	610	575	535	498	456	412	362	322	345	388
N4	695	602	597	650	716	778	816	865	902	914	938	923	911	876	844	797	771	700	651	572	513	455	432	449	517
N5	541	476	454	497	538	579	636	664	689	711	704	675	675	670	642	606	561	505	454	405	363	309	299	321	348
N6	428	376	370	402	446	478	528	540	563	574	576	578	574	558	536	495	463	410	378	336	294	258	240	255	288
O1	350	315	325	348	373	414	451	487	505	520	520	515	510	505	493	469	451	414	381	350	322	285	248	265	294
O2	373	318	320	351	386	434	455	484	505	526	528	540	521	515	502	487	471	435	390	355	322	290	248	248	286
O3	346	380	447	491	560	626	685	727	768	802	812	842	840	835	832	805	756	730	681	622	547	479	436	385	312
O4	725	632	620	685	729	802	861	914	952	964	965	955	948	908	872	858	812	730	666	600	532	466	420	423	482
O6	518	471	456	492	534	594	646	670	678	670	670	670	655	630	600	576	528	484	423	385	333	294	261	264	295
O7	357	329	307	321	349	396	417	432	453	458	458	470	452	441	422	410	382	352	324	290	265	231	211	212	243
P1	390	348	339	382	418	449	497	524	545	548	558	554	555	540	519	495	464	451	408	375	326	290	268	290	322
P2	652	575	537	561	646	713	776	793	833	858	868	875	861	835	805	772	720	671	630	569	510	444	400	395	451
P3	481	420	416	436	490	530	575	600	615	618	625	610	605	590	565	520	485	452	400	371	336	306	280	294	328
P4	688	569	569	626	684	739	793	833	890	910	914	911	910	890	850	806	752	714	652	595	533	470	432	456	474
P5	682	615	579	622	672	734	805	832	914	933	956	965	902	887	826	800	748	685	636	562	500	435	380	392	442
P6	556	480	468	505	565	608	665	686	704	716	734	715	708	691	656	638	563	528	488	440	381	335	308	318	358
P7	308	270	270	276	313	333	356	373	380	385	370	366	364	360	340	316	300	281	256	236	204	180	161	170	200
Q1	377	326	326	348	383	425	475	494	497	510	516	526	522	502	483	459	422	404	385	340	304	270	245	276	303
Q2	540	462	468	495	538	601	629	645	670	694	688	688	679	650	628	591	540	502	466	421	365	321	289	294	345
Q4	708	631	636	700	771	835	886	900	927	945	942	932	924	880	832	722	710	637	580	520	441	407	372	416	461
Q5	386	442	503	561	635	690	762	808	854	883	920	938	943	945	932	900	871	823	770	700	606	535	466	391	322
Q6	488	439	413	450	496	529	573	606	641	650	646	640	639	620	585	548	534	485	448	405	369	320	280	291	327
R2	398	356	342	360	413	442	478	511	516	530	535	541	531	516	494	461	438	309	383	346	306	286	241	245	283
R3	468	404	377	403	432	482	524	550	565	572	589	578	567	544	517	491	471	426	397	360	310	278	244	248	286
R4	651	575	540	565	628	691	758	805	825	840	839	835	824	808	781	740	694	644	600	540	490	430	370	366	434
R5	560	491	485	531	578	628	673	710	735	751	752	758	748	735	711	675	640	599	546	490	449	400	363	369	425
R6	386	345	338	365	408	441	478	493	515	534	630	522	510	499	478	473	447	416	382	350	312	277	250	262	288
S3	338	300	297	326	350	384	416	430	458	466	465	459	456	446	424	413	395	356	328	303	271	240	217	220	267
S4	394	344	335	356	400	445	474	496	519	531	543	555	528	517	498	475	458	430	391	350	303	278	255	268	312
S5	332	299	291	308	349	375	408	433	448	468	465	465	459	443	425	400	388	355	327	300	269	241	221	221	265

The neutron flux measurements for the refined method are listed in Table X. All the results are listed as saturated activity. The use of this table is explained in Section 4.4.3.2.

4.4.3.1 Determination of Core Power by the Standard Method

Experimental measurements have shown that 193 Mev of energy is released per fission (Ref. 3). Thus the power generated in an element, or core, is reduced to evaluation of the fission rate. Since the fission rate is proportional to the thermal-neutron flux, the power could be computed if the thermal flux were everywhere known. It is impossible to measure flux at each point in the reactor; hence, some compromise and averaging assumptions must be made. One method, the standard method, consists of the steps outlined below.

1. Irradiate a bare gold foil at the center of each fuel element (location 310 on Figure 32).
2. Irradiate a cadmium-covered foil at location 310 of each fuel element.
3. Compute saturated activities of each foil. Calculate thermal saturated activity by subtracting cadmium-covered S.A. from bare S.A.
4. Convert thermal saturated activity to thermal-neutron flux by the formula

$$\phi_{th} = \frac{S.A.th}{\sigma \cdot 60},$$

where

$$\phi = \text{thermal-neutron flux, } \frac{\text{neut}}{\text{cm}^2\text{-sec}};$$

$$S.A.th = \text{thermal saturated activity, } \frac{\text{disintegrations}}{\text{min-gm}};$$

$$\sigma = \text{cross-section for gold} = 0.294 \frac{\text{cm}^2}{\text{gm}}; \text{ and}$$

$$60 = \text{conversion factor for seconds to minutes.}$$

TABLE X
NEUTRON FLUX MEASUREMENTS IN LATTICE LOCATIONS

Foil Location Code	Q2	O4	S4	R6	P7	P6	P4	N2	N4	R5	Q6
110	.155**	.203	.142	.132	.897(9)	.185	.230	.167	.191	.177	.130
111	.153	.245	.118	.124	.698(9)	Lost	.239	.189	.211	.161	.141
112	.152	.260	.132	.150	.120	.169	.227	.163	.210	.180	.189
113	.192	.213	.162	.134	.989(9)	.145	.233	.162	.181	.210	.151
114	.114	.134	.127	.104	.808(9)	.121	.214	.194	.174	.150	.712(9)
210	.238	.375	.220	.206	.142	.289	.377	.259	.285	.272	.175
211	.270	.429	.240	.254	.134	.269	.436	.338	.383	.254	.244
212	.265	.525	.223	.261	.222	Lost	.399	.371	.355	.302	.393
213	.355	.385	.286	.231	.180	.267	.442	.335	.315	.424	.266
214	.225	.267	.221	.212	.175	.211	.396	.359	.293	.250	Lost
310	.434	.546	.304	.292	.212	.420	.525	.385	.423	.437	.264
311	.397	.662	.333	.359	.203	.387	.633	.461	.587	.356	.350
312	.377	.738	.319	.354	.306	.466	.580	.459	.496	.425	.564
313	.509	.575	.404	.354	.275	Lost	.633	.457	.437	.603	.396
314	.511	.576	.304	.299	.231	.306	.569	.449	.455	.362	.294
410	.481	.525	.272	.279	.206	.403	.447	.323	.392	.358	.315
411	.379	.599	.294	.318	.258	.381	.549	.404	.512	.317	.323
412	.353	.659	.273	.312	.289	.434	.543	.391	.440	.407	.520
413	.465	.512	.365	.323	.261	.394	.549	.396	.387	.555	.373
414	.562	.636	.267	.296	.234	.298	.504	.388	.416	.312	.321
510	.324	.327	Lost	.202	.147	.287	.316	.205	.273	.254	.184
511	.242	.360	.155	.175	Lost	.235	.226	.244	.328	.203	.212
512	.228	.372	.179	.209	.205	.306	.329	.217	.283	.272	.287
513	.291	.327	.226	.197	.158	.252	.332	.204	.240	.289	.246
514	.339	.378	.169	.156	.139	.204	.324	.254	.280	.210	.205
110(Cd)*	.337(9)	.387(9)	.259(9)	.249(9)	.388(9)	.309(9)	.507(9)	.222(9)	.353(9)	.315(9)	.302(9)
310(Cd)	.133	.185	.102	.105	.941(9)	.138	.197	.141	.162	.143	.103
510(Cd)	.454(9)	.725(9)	.404(9)	.363(9)	.606(9)	.612(9)	.604(9)	.402(9)	.587(9)	.707(9)	.495(0)

*All values multiplied by 10¹⁰, unless otherwise noted.

**Denotes cadmium-covered foil activation.

5. Irradiate a copper wire along the axial centerline of each fuel element. Count the relative activity. Find the average activity along the 24 inches of active fuel area.
6. Compute the ratio of average activity to activity at location of foils in Steps 1 and 2. Call this α , the average-to-maximum ratio.
7. Compute the average thermal-neutron flux in each element by multiplying α by ϕ from Step 4. Call this ϕ_1 .
8. Compute core average thermal-neutron flux by

$$\phi_c = \frac{1}{32} \sum_{i=1}^{32} \phi_i,$$

where

ϕ_c = core average thermal-neutron flux, and

ϕ_i = average thermal-neutron flux in i^{th} location.

9. Compute core power by the following formula:

$$P = K \overline{\sigma_f} \frac{N}{A} M \rho_e \phi_c,$$

where

$K = 3.088 \times 10^{-11}$ watt-sec/fission,

σ_f = average fission cross section for $U^{235} = 487b$,

$N = 0.6023 \times 10^{24}$,

$A = 235$,

M = mass of $U^{235} = 4800$ gm for 32 full elements,

$\rho_e = 1.107$ (see references 3 and 4), and

ϕ_c = from Step 8 above.

Thus $P = 2.054 \times 10^{-7} \phi_c$. The core power is then computed from this formula.

Often only the percentage power contribution for each lattice location is desired. In this case, the following procedure is followed:

10. Repeat Steps 1, 2, 3, 5, and 6 above.
11. Find the average thermal saturated activity for each location by

$$S.A. \text{ avg} = S.A. \text{ th} \cdot \alpha ,$$
 where

$$S.A. \text{ avg} = \text{the average thermal saturated activity.}$$
12. Calculate the percentage contribution, r_i , by

$$r_i = \frac{(S.A. \text{ avg})_i}{\sum_{i=1}^{32} (S.A. \text{ avg})_i} ,$$

where i denotes the i^{th} location.

This procedure was followed in this report. The results are listed in Table VIII.

4.4.3.2 A Refinement for Calculation of Core Power

One basic error of the standard method is that it implicitly assumes that there is no radial gradient of neutron flux within the element. For example, the single foil location of 310 implies that the flux in the 3-row (locations 310, 311, 312, 313, and 314) is constant. Other experiments (Ref. 5) have shown this to be untrue.

A refinement method was devised and is outlined below.

1. Proceed as listed in Steps 10 through 12 of Section 4.1 to find average thermal saturated activity for each location.
2. Make symmetry assumptions (Fig. 34).

3. Irradiate bare gold foils at each of 25 selected locations (Fig. 33) in one element of each symmetrical group (12 in all).
4. Irradiate cadmium-covered foils at the 110 and 510 locations of each selected location. (The 210 and 410 locations are omitted, since the cadmium ratio does not change materially from that at the 310 location previously measured.)
5. Carry out the following procedure for determining the average saturated activity in each of the 12 elements
 - a. Find the cadmium ratio for the 1-row by the formula

$$\text{C.R.} = \frac{(\text{S.A. bare})_{110}}{(\text{S.A. Cd})_{110}}.$$
 - b. Find the average saturated activity for the 1-row by

$$\text{S.A. avg} = \frac{1}{5} (\text{S.A.}_{110} + \text{S.A.}_{111} + \dots + \text{S.A.}_{114}).$$
 - c. Find the average thermal saturated activity for the 1-row by

$$(\text{S.A. th})_{\text{avg}} = \frac{\text{C.R.} - 1}{\text{C.R.}} \times \text{S.A. avg}.$$
 - d. Repeat for the 2-, 3-, 4-, and 5-rows. For the C.R. of the 2- and 4-rows, use that of the 3-row.
 - e. Assume that the average thermal saturated activity for the first three inches of fuel can be calculated from the formula

$$\beta_A = \frac{R_A}{R_1} \cdot (\text{S.A.})_1,$$

where

R_A = average wire activity for first 3 inches (Table IX),

R_1 = wire activity at 0 inches (also Table IX),

S.A.1 = from Step c above, and

β_A = average thermal saturated activity for first 3 inches.

- f. Find the fuel from 3 inches to 9 inches from the aft end, find the average thermal saturated activity by

$$\beta_A = \frac{R_B}{R_2} \cdot S.A.2,$$

where

R_B = average wire activity from 3 inches to 9 inches

R_2 = wire activity at 6 inches

S.A.2 = $\left(\frac{C.R.-1}{C.R.}\right) (S.A.210 + \dots + S.A.214)$, and

β_B = average thermal saturated activity.

- g. Repeat Step f for the 3- and 4-rows.
h. Repeat Step e for the 5-row.
j. Calculate the average thermal saturated activity for the element by the formula

$$\beta_{avg} = \frac{3\beta_A + 6\beta_B + 6\beta_C + 6\beta_D + 3\beta_E}{24}.$$

This gives the refined results listed in Table XI.

- k. Since only one element in each symmetrical group has a refined result, calculate a connection factor, K, for each group

$$K = \frac{\text{refined result}}{\text{standard result (Table VIII)}}$$

- m. Correct the standard result in each group by multiplying the correction factor for that group.
n. Compute the percentage contribution as in Step 12, Section 4.4.3.1.

- o. Compute flux/watt per element by the formula

$$(\text{flux/watt}) = \frac{\frac{2.054 \cdot 10^{-7}}{32} \sum_{i=1}^{32} \frac{\alpha_i (0.294)(60)}{(0.294)(60)}}{(0.294)(60)}$$

The results from Steps j, k, m, n, o are listed in Table XI.

4.4.3.3 Radial Flux Changes in Individual Lattice Locations

Several interesting results were obtained from the refined method. For example, a comparison of saturated activities in the 3-row of Q-6 shows the following:

<u>Location</u>	<u>Saturated Activity</u> 10^{10}
310	0.264 (center)
311	0.350 (next to fuel element)
312	0.564 (next to dummy)
313	0.396 (next to fuel element)
314	0.294 (next to rod location)

The average of these five numbers is 0.374, or 42% higher than the center measurement. This example shows the inherent inaccuracy of using the standard method.

Another interesting result is the comparison of the following columns:

<u>Location</u>	<u>Activity</u>	<u>Activity</u>	<u>Location</u>
P-6 114	0.121	0.120	P-7 112
214	0.211	0.222	212
314	0.306	0.306	312
414	0.298	0.289	412
514	0.204	0.205	512

Inspection of Figures 33 and 34 revealed that the 4-column of P-6 and the 2-column of P-7 are the same line in the reactor. The

TABLE XI
POWER GENERATION AS DETERMINED BY REFINED METHOD

ASTR Lattice Location	Refined Average Thermal Saturated Activity (x 1010) (dpm/gm-w)	Average Thermal Saturated Activity (x 1010) (From Table I) (dpm/gm-w)	K	Corrected Average Thermal Saturated Activity (x 1010) (dpm/gm-w)	Element Contribution (%)	Average Thermal Flux per Watt (x 106) (n/cm ² -sec-w)
M3	-	.162	1.1606	.188	2.74	4.28
M4	-	.156	1.0186	.159	2.32	3.62
M5	-	.144	1.1606	.167	2.44	3.80
N2	0.224	.193	-	.224	3.27	5.10
N3	-	.233	1.2685	.296	4.32	6.73
N4	0.234	.236	-	.234	3.41	5.32
N5	-	.187	1	.187	2.73	4.25
N6	-	.169	1.1606	.196	2.86	4.46
O1	-	.193	1.1606	.224	3.27	5.10
O2	-	.252	1.2685	.320	4.67	7.28
O4	0.318	.312	-	.318	4.64	7.23
O6	-	.158	1	.158	2.31	3.59
O7	-	.099	1.1606	.114	1.66	3.78
P1	-	.245	1.0186	.250	3.65	5.69
P2	-	.198	0.9915	.196	2.86	4.46
P3	-	.302	1.0192	.308	4.49	7.01
P4	0.288	.263	-	.288	4.20	6.55
P5	-	.233	1.0192	.237	3.46	5.39
P6	0.205	.222	-	.205	2.99	4.66
P7	0.115	.081	-	.115	1.68	2.62
Q1	-	.179	1.1606	.208	3.03	4.73
Q2	0.222	.222	-	.222	3.24	5.05
Q4	-	.242	1.0192	.247	3.60	5.62
Q6	0.191	.148	-	.191	2.79	4.35
R2	-	.202	1.1606	.234	3.41	5.32
R3	-	.216	1	.216	3.15	4.91
R4	-	.210	0.9915	.208	3.03	4.73
R5	0.222	.175	-	.222	3.24	5.05
R6	0.170	.147	-	.170	2.48	3.87
S3	-	.176	1.1606	.204	2.98	4.64
S4	0.164	.161	-	.164	2.39	3.73
S5	-	.156	1.1606	.181	2.64	4.12

fact that the numbers were very close even though the foils were irradiated on separate runs is good testimony to the experimental accuracy. Other similarities were also noted in adjacent columns.

A portion of the data in Table X was reduced to thermal-neutron flux per watt in order to illustrate the variation of flux within the core. The illustrated portions are:

1. The thermal flux profile across the O-row @ core midplane (Fig. 35).
2. The thermal flux profile across the 4-row @ core midplane (Fig. 36).
3. The thermal flux profile across the P-row @ core midplane (Fig. 37).

Also reduced to thermal flux/watt was the axial flux in lattice location O-4 (Table XII and Fig. 38).

TABLE XII
AXIAL FLUX PROFILE FOR LATTICE LOCATION O-4

Row	Thermal Flux/Watt ($\frac{\text{neutrons}}{\text{cm}^2\text{-sec-w}}$) x 10 ⁶				
	Column				
	10	11	12	13	14
1	3.73	4.50	4.78	3.91	2.46
2	5.35	6.12	7.48	5.48	3.80
3	8.21	9.42	10.51	8.19	8.19
4	7.48	8.53	9.40	7.30	9.05
5	5.78	6.37	6.57	5.78	6.69

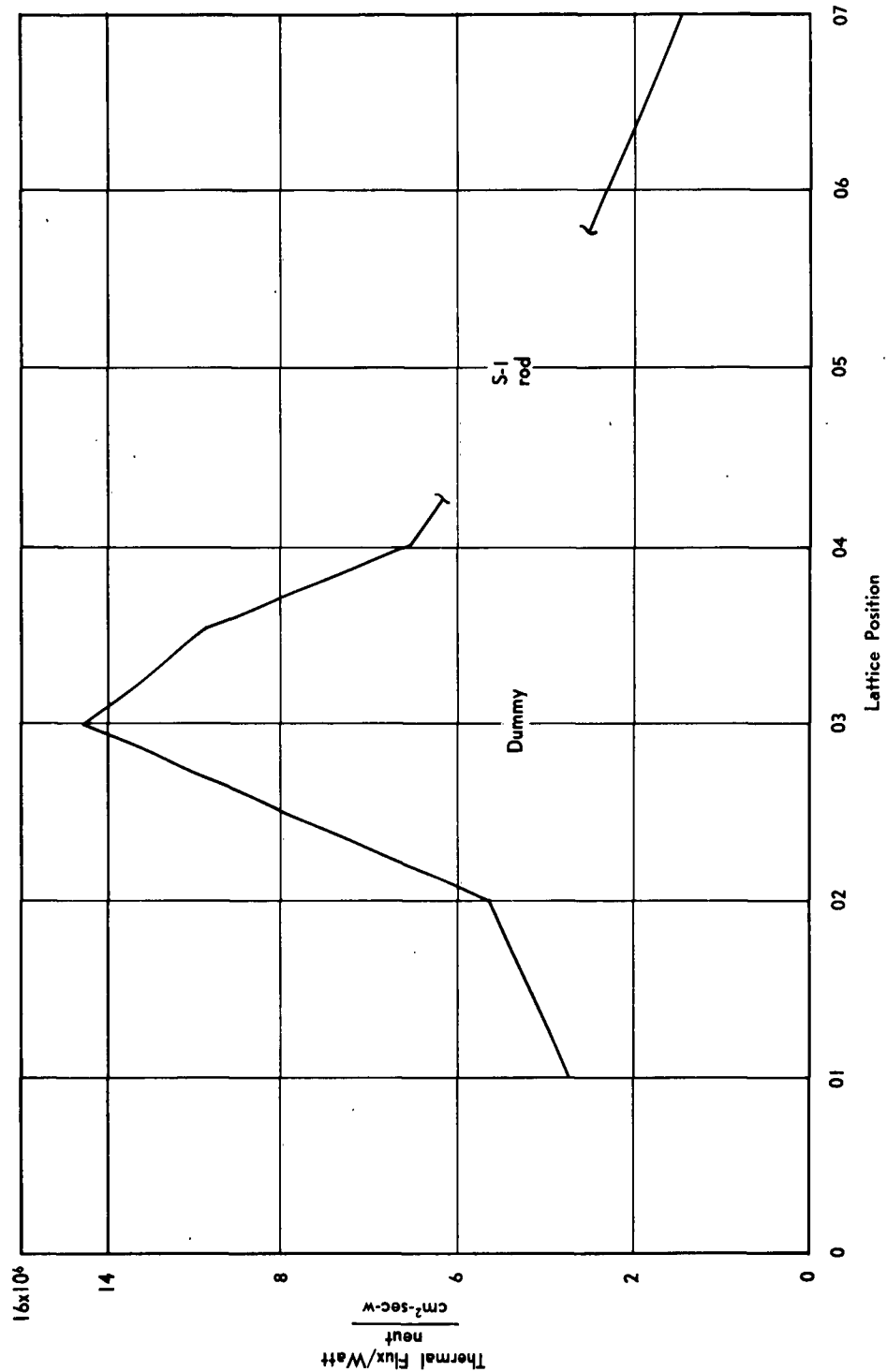


FIGURE 35. Flux Profile across O-Row at Midplane

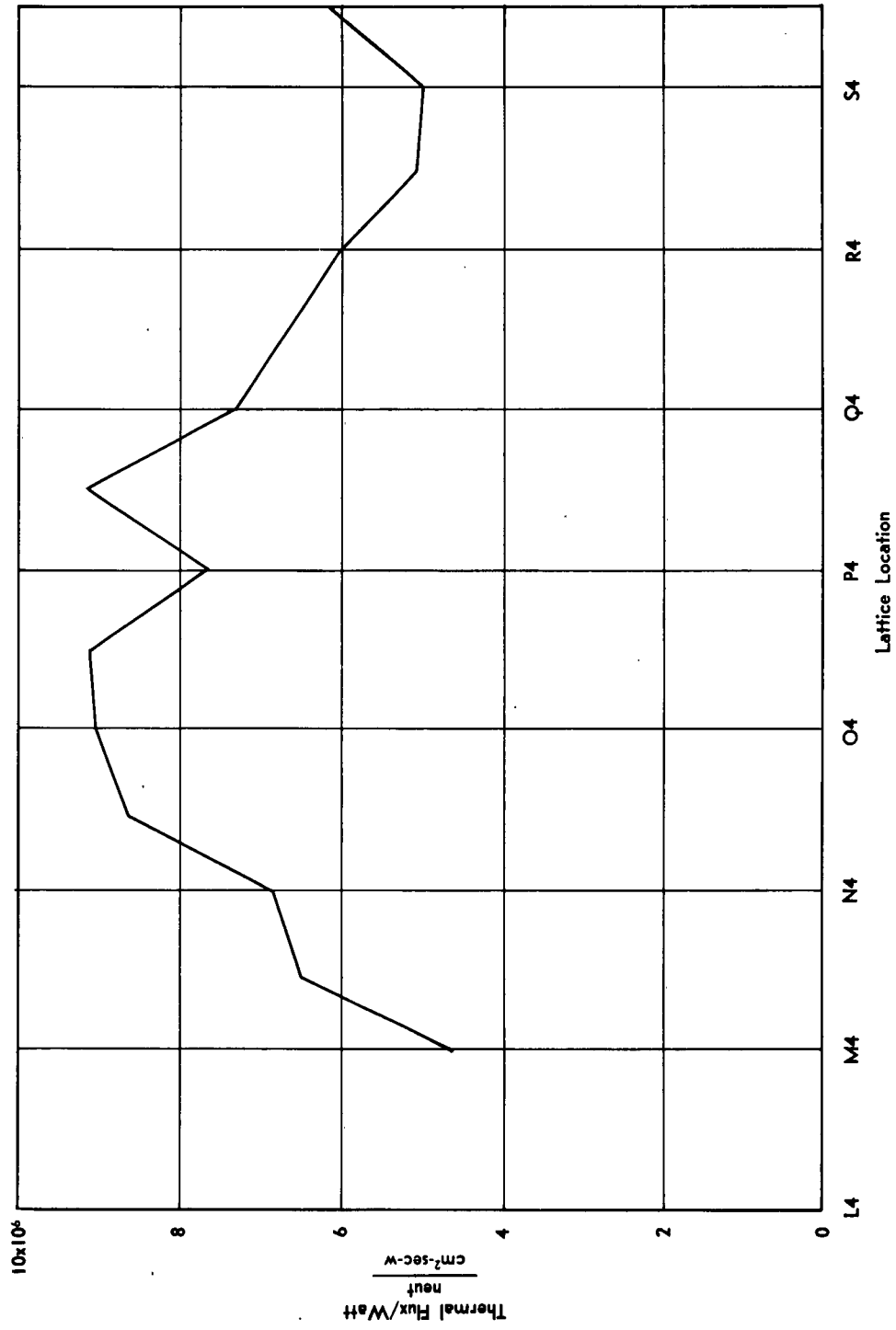


FIGURE 36. Flux Profile across 4-Row at Midplane

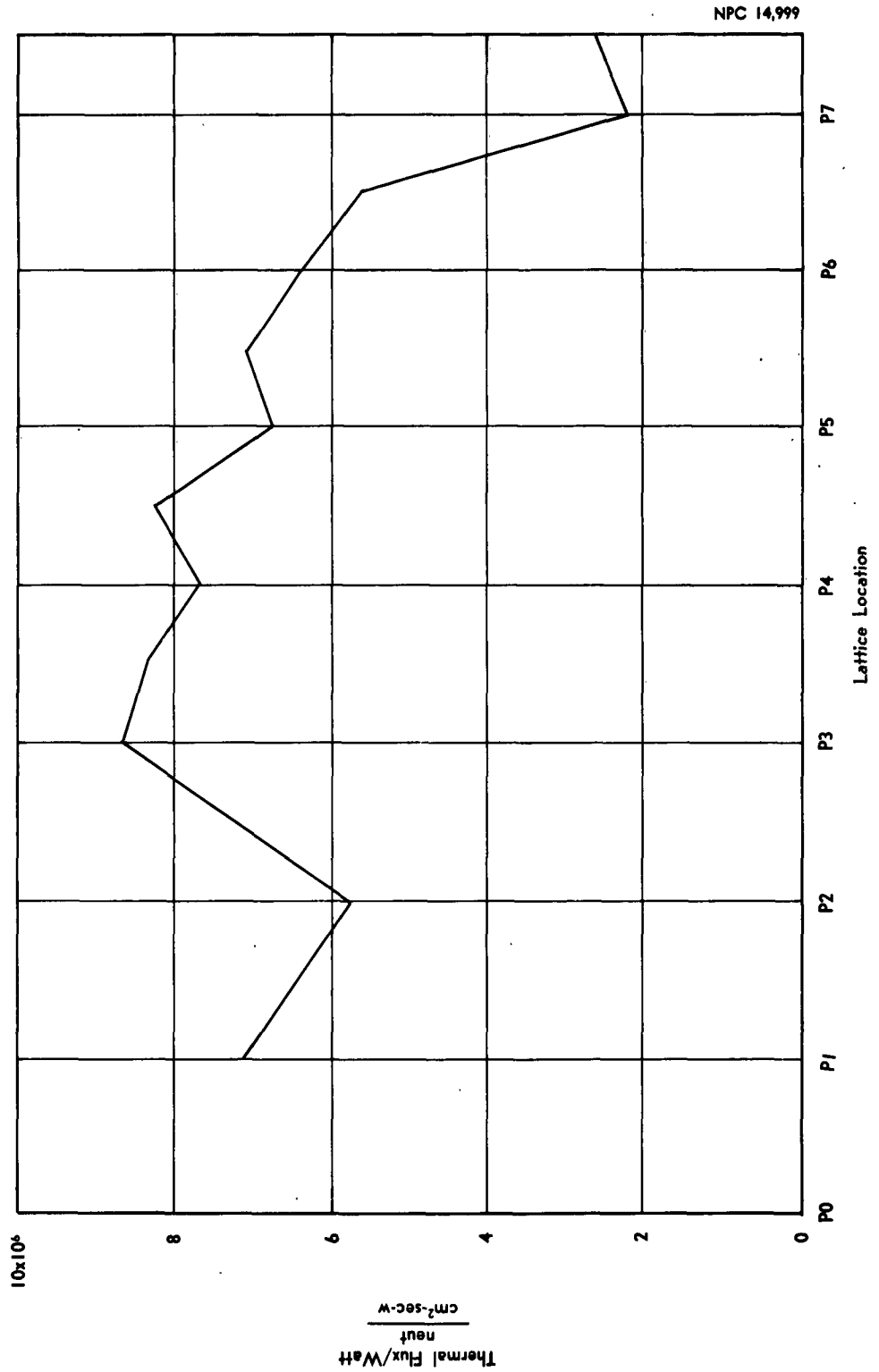


FIGURE 37. Flux Profile across P-Row at Midplane

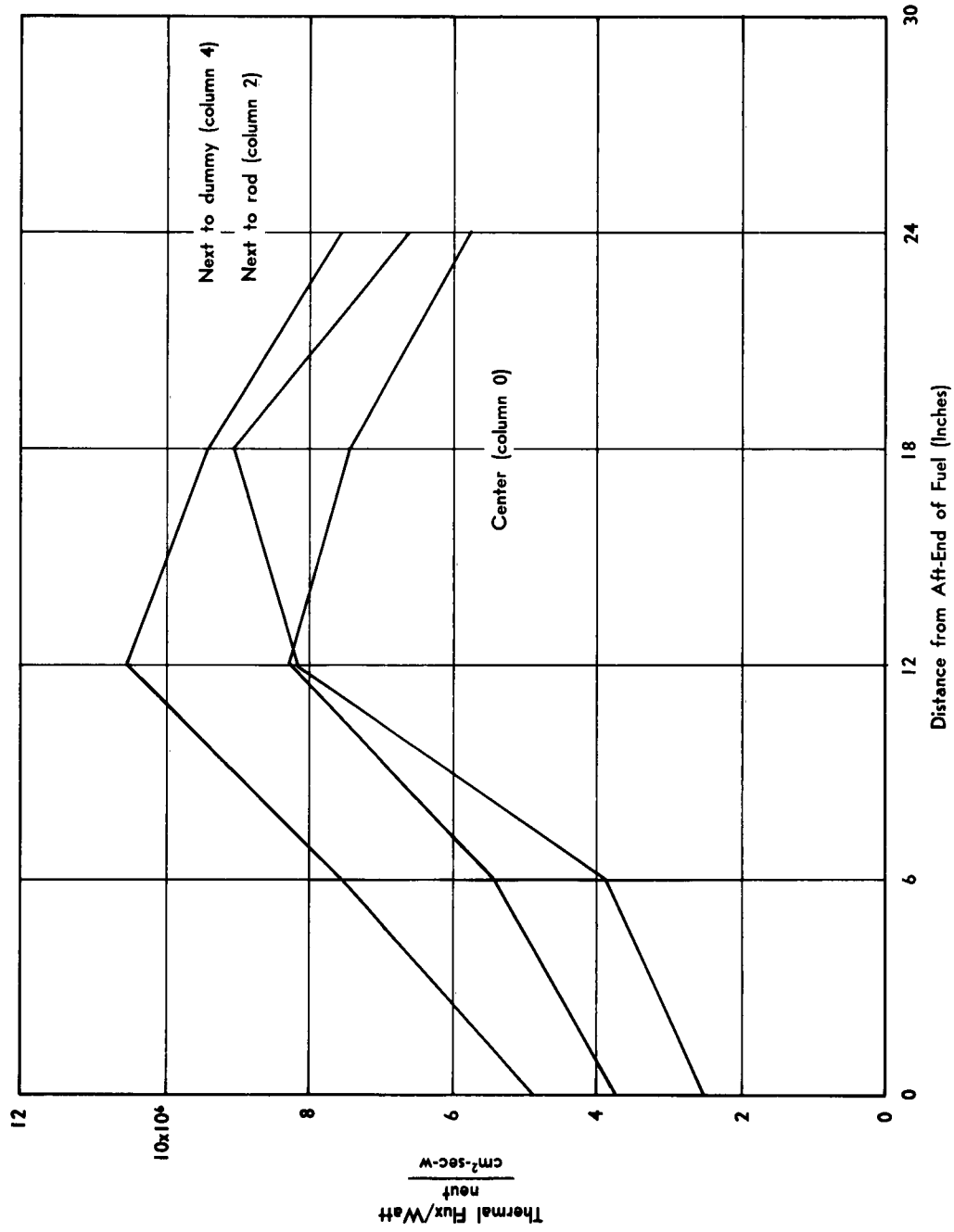


FIGURE 38. Axial Flux Profile for Lattice Location O-4

The influence of a dummy element can be seen in Figure 35. The decrease of flux in the center of an element is shown in Figures 36 and 37. The influence of a rod adjacent to an element is shown in Figure 38; the flux is depressed in the vicinity of the rod and amplified where rod has been withdrawn.

REFERENCES*

1. 3-Mw ASTR. General Dynamics/Fort Worth Report FZK-9-161 (18 August 1961).U
2. Ross, D. F., Optimization of Reactor Coolant Flow for the Aircraft Shield Test Reactor. General Dynamics/Fort Worth Report MR-N-261 (October 1960).U
3. Hazards Summary Report for the Reactivity Test Assembly. General Dynamics/Fort Worth Report FZK-9-153 (8 August 1960).U
4. Determination of the Power of the Bulk Shielding Reactor - Part III Measurement of the Energy Released per Fission. Oak Ridge National Laboratory Report ORNL-1537 (11 March 1954).U
5. Low-Power Calibration of GTR, Convair-Fort Worth Report FZK-9-075 (CVAC-228T, 18 June 1954). U
6. Thermal-Neutron Flux Measurement at the MTR-ETR Site. Idaho Operations Office Report IDO-16538 (28 October 1960). U

* All General Dynamics/Fort Worth reports published before July 1961 are referenced as Convair-Fort Worth reports.

DISTRIBUTION

FZK-9-179

1 February 1963

<u>Addressee</u>	<u>No. of Copies</u>
ASRCNL	2
ASRCPR-2	2
ASRMCE-1	2
ASRMPE-2	2
ASBMPT	2
ASTEN	1
ASAPRD-NS	3
GD/Convair	1
Convair-ASTRO	2
TIS	20
Lockheed-Ga.	1
Boeing AFPR	1
Douglas, Dept. A26	1
North American	1
Pratt and Whitney	1
ORNL	1
NDA	1
Naval Ord. Lab	1
Battelle-REIC	1
Air Univ. Lib.	1
Radioplane	1
Republic Avia.	1
Vought-Aero	1
AFSWC (Tech. Inf)	1
NASA-MSFC	1
NASA-Wash.	1
NASA-Lewis	1
AFPR-RCRFE	1
AFRDC-AE	1
ASZX	2
ASTIA	10

<p>Nuclear Aerospace Research Facility, General Dynamics/Fort Worth, Fort Worth, Texas. THE FIRST OPERATIONAL YEAR OF THE RTA, by J. T. Pancoast and E. L. Jordan. 1 February 1963. 103p. incl. illus., tables, 6 refs. (NARF-62-14T; FZK-9-179)</p> <p>Contract AF33(657)-7201 Unclassified report</p> <p>On 24 January 1961 the Reactivity Test Assembly (RTA) - a heterogeneous, light-water, unpresurized, fully enriched system that operates as a zero-power reactor - at General Dynamics/Fort Worth was brought critical for the first time. During the year following, the RTA was used in 11 major experiments that covered the operational testing and continued research for the two 3-Mw reactors at the Nuclear Aerospace Research Facility at GD/FW.</p>	<p>UNCLASSIFIED</p> <ol style="list-style-type: none">1. Nuclear reactors, *Critical assemblies, Reactor *reactivity, Control rods2. Reactor *operations, Experimental data3. Reactor control, Neutron detectors4. Ground Test Reactor (GTR), Aerospace Systems Test Reactor (ASTR), Reactivity Test Assembly (RTA) <p>I. Pancoast, J. T. II. Jordan, E. L. III. Aeronautical Systems Division, Air Force Systems Command IV. Contract AF33(657)-7201</p> <p>UNCLASSIFIED</p>
<p>Nuclear Aerospace Research Facility, General Dynamics/Fort Worth, Fort Worth, Texas. THE FIRST OPERATIONAL YEAR OF THE RTA, by J. T. Pancoast and E. L. Jordan. 1 February 1963. 103p. incl. illus., tables, 6 refs. (NARF-62-14T; FZK-9-179)</p> <p>Contract AF33(657)-7201 Unclassified report</p> <p>On 24 January 1961 the Reactivity Test Assembly (RTA) - a heterogeneous, light-water, unpresurized, fully enriched system that operates as a zero-power reactor - at General Dynamics/Fort Worth was brought critical for the first time. During the year following, the RTA was used in 11 major experiments that covered the operational testing and continued research for the two 3-Mw reactors at the Nuclear Aerospace Research Facility at GD/FW.</p>	<p>UNCLASSIFIED</p> <ol style="list-style-type: none">1. Nuclear reactors, *Critical assemblies, Reactor *reactivity, Control rods2. Reactor *operations, Experimental data3. Reactor control, Neutron detectors4. Ground Test Reactor (GTR), Aerospace Systems Test Reactor (ASTR), Reactivity Test Assembly (RTA) <p>I. Pancoast, J. T. II. Jordan, E. L. III. Aeronautical Systems Division, Air Force Systems Command IV. Contract AF33(657)-7201</p> <p>UNCLASSIFIED</p>
<p>Nuclear Aerospace Research Facility, General Dynamics/Fort Worth, Fort Worth, Texas. THE FIRST OPERATIONAL YEAR OF THE RTA, by J. T. Pancoast and E. L. Jordan. 1 February 1963. 103p. incl. illus., tables, 6 refs. (NARF-62-14T; FZK-9-179)</p> <p>Contract AF33(657)-7201 Unclassified report</p> <p>On 24 January 1961 the Reactivity Test Assembly (RTA) - a heterogeneous, light-water, unpresurized, fully enriched system that operates as a zero-power reactor - at General Dynamics/Fort Worth was brought critical for the first time. During the year following, the RTA was used in 11 major experiments that covered the operational testing and continued research for the two 3-Mw reactors at the Nuclear Aerospace Research Facility at GD/FW.</p>	<p>UNCLASSIFIED</p> <ol style="list-style-type: none">1. Nuclear reactors, *Critical assemblies, Reactor *reactivity, Control rods2. Reactor *operations, Experimental data3. Reactor control, Neutron detectors4. Ground Test Reactor (GTR), Aerospace Systems Test Reactor (ASTR), Reactivity Test Assembly (RTA) <p>I. Pancoast, J. T. II. Jordan, E. L. III. Aeronautical Systems Division, Air Force Systems Command IV. Contract AF33(657)-7201</p> <p>UNCLASSIFIED</p>
<p>Nuclear Aerospace Research Facility, General Dynamics/Fort Worth, Fort Worth, Texas. THE FIRST OPERATIONAL YEAR OF THE RTA, by J. T. Pancoast and E. L. Jordan. 1 February 1963. 103p. incl. illus., tables, 6 refs. (NARF-62-14T; FZK-9-179)</p> <p>Contract AF33(657)-7201 Unclassified report</p> <p>On 24 January 1961 the Reactivity Test Assembly (RTA) - a heterogeneous, light-water, unpresurized, fully enriched system that operates as a zero-power reactor - at General Dynamics/Fort Worth was brought critical for the first time. During the year following, the RTA was used in 11 major experiments that covered the operational testing and continued research for the two 3-Mw reactors at the Nuclear Aerospace Research Facility at GD/FW.</p>	<p>UNCLASSIFIED</p> <ol style="list-style-type: none">1. Nuclear reactors, *Critical assemblies, Reactor *reactivity, Control rods2. Reactor *operations, Experimental data3. Reactor control, Neutron detectors4. Ground Test Reactor (GTR), Aerospace Systems Test Reactor (ASTR), Reactivity Test Assembly (RTA) <p>I. Pancoast, J. T. II. Jordan, E. L. III. Aeronautical Systems Division, Air Force Systems Command IV. Contract AF33(657)-7201</p> <p>UNCLASSIFIED</p>